PHOTOCATALYTIC STUDIES OF $Cs_2AgIn_{(1-x)}Sb_xCl_6$ SYNTHESIZED USING ACID PRECIPITATION METHOD

A Dissertation Report for

PHGO-311 Dissertation

Credits: 8

Submitted in partial fulfillment of

Master of Science

in

Physics

by

MS. SONALI SINGH

Roll No: 21P043044

Under the Supervision of

DR. VENKATESHA R. HATHWAR

School of Physical and Applied Sciences
Goa University

Goa University

MAY 2023

Examined by:

Seal of the School

DECLARATION BY STUDENT

I hereby declare that the data presented in this Dissertation, "Photocatalytic Studies of $Cs_2AgIn_{(1-x)}Sb_xCl_6$ Synthesized using Acid Precipitation Method" is based on the results of investigations carried out by me in the Goa University at the School of Physical and Applied Sciences, Goa University under the supervision of Dr. Venkatesha R. Hathwar, Assistant Professor, and the same has not been submitted elsewhere for the award of a degree or diploma by me. Further, I understand that Goa University or its authorities will not be responsible for the correctness of observations/experimental or other findings given the dissertation.

I hereby authorize the University authorities to upload this dissertation on the dissertation repository or anywhere else as the UGC regulations demand and make it available to anyone as needed.

Singh

Ms. Sonali Singh
21P043044
Goa University
School of Physical and Applied Sciences

Date: 10-05-2023

Place: Goa University

COMPLETION CERTIFICATE

This is to certify that the dissertation report "**Photocatalytic Studies of $Cs_2AgIn_{(1-x)}Sb_xCl_6$ Synthesized using Acid Precipitation Method**" is a bonafide work carried out by Ms. Sonali Singh under my supervision in partial fulfilment of the requirements for the award of the degree of **Physics** in the Discipline Goa University at the School of Physical and Applied Sciences Goa University.

Dr.Venkatesha R. Hathwar
Assistant Professor
Goa University

Date: 10-05-2023

School Stamp

Dr. Kaustubh R.S Priolkar

Goa University

Dean School of Physical and Applied Sciences

Date:

Place: Goa University

ACKNOWLEDGEMENT

It gives me a great sense of pleasure to present the report of the project work undertaken during MSc final year. Although I have worked hard for the success of this project, it wouldn’t have been possible without some people who have helped and guided me throughout the course of my work. So, I would like to express a deep sense of gratitude to those people.

First, I would like to thank my project guide Dr. Venkatesha R. Hathwar sir for his excellent guideship and intelligence. Thank you sir for always motivating and inspiring me.

I would like to thank Mr. Irshad Shaikh sir for his constant help and support throughout the project work. Thank you so much sir for being a great guide and friend.

I thank all the PhD students of physics who have helped me by explaining how to use different instruments and software.

I also want to thank the School of Physical and Applied Sciences for providing me with all the required instruments for my project work.

My sincere thanks to all faculties of physics for providing me with the conceptual knowledge needed.

I express my gratitude towards my family for their kind encouragement and appreciation throughout.

Also special thanks to Mr. Alister Faby Cardozo for constantly motivating and supporting me throughout this journey.

Lastly, I want to thank my MSc friends who made work time joyful but always efficient.

Abstract

Lead halide perovskites have intrigued many due to their photocatalytic applications in recent times. They can act as efficient photocatalysts for a range of chemical reactions. This is due to their ability to absorb light over a wide range of wavelengths However, the poor stability, lead toxicity and the low photocatalytic activity of lead halide perovskites are preventing these defect-tolerant materials from wide applications in photocatalysis. Therefore a lead free halide based double perovskites (DP), $Cs_2AgInCl_6$ which is a semiconductor with direct band gap (~3.33 eV) have emerged to be the most promising green and efficient oxidation one by using renewable solar energy to carry out photocatalysis. The octahedral $Cs_2AgInCl_6$ DP particles were prepared by precipitation from acid solutions. The as prepared sample has the potential to degrade water-insoluble carcinogens over time. $Cs_2AgInCl_6$ degraded Sudan Red III dye in 120 mins and Methyl Orange in 180 mins.

Contents

List of figures

1. Introduction

1.1 Organic pollutants

The world appears to be an aesthetic place due to the colors that are present around us. The use of color has become an important part of human culture and lifestyle, both in nature and in the products we create. From the bright colors of flowers and birds to the colorful paintings and textiles of human art, color plays a vital role in our perception of the world around us. With the rise of industrialization, the use of color has become even more prevalent as industries have sought to enhance the appearance of their products to attract customers and increase sales. This has led to the development of a wide range of synthetic dyes and pigments, which can be used to produce a vast array of colors and shades.[1]

The use of color in industrial products has also become an important tool for branding and marketing. Companies often use specific colors in their logos and packaging to create a recognizable brand identity and appeal to specific target markets. However, water pollution due to organic dye waste from industries is a serious environmental problem that can have significant negative impacts on aquatic ecosystems and human health. One of which is the discoloration of water, which can affect the aesthetic quality of water and make it less appealing for recreational activities such as swimming or fishing. Organic dyes can also be toxic to aquatic life, and can disrupt the food chain by killing or impairing fish and other aquatic organisms.[2]

In particular, the use of toxic organic dyes and their intermediates by industries such as paint, varnish, textiles, plastics, ink, and cosmetics can have severe consequences for the environment. These dyes are often difficult to remove from wastewater and can persist in the environment for long periods of time, leading to contamination of water bodies and soil.[3] It is therefore important for industries to take responsibility for the environmental and health impacts of their production processes and to work towards minimizing their use of harmful pollutants.

1.2 What are dyes?

Dyes are substances capable of imparting color by chemically or physically binding with materials.

Unlike most organic compounds, dyes possess colour because they

1) absorb light in the visible spectrum (400–700 nm),

2) have at least one chromophore (colour-bearing group),

3) have a conjugated system, i.e. a structure with alternating double and single bonds, and

4) exhibit resonance of electrons, which is a stabilizing force in organic compounds [4]

While the quality of dyes varies with the manufacturer, the dyes which take less time to colour the fabric and are chemically stable are most preferable. Dying the fabric forms strong chemical bonds between dye molecules and the fabric. Temperature and time are two important factors that determine the durability of the dye

There are various types of organic dyes that are commonly used in industries for coloring and printing purposes. Some of the most common types of organic dyes include:

Azo dyes: These dyes are the most widely used organic dyes and are commonly used in the textile and leather industries. They are derived from the azo group (-N=N-) and can have a range of colors.

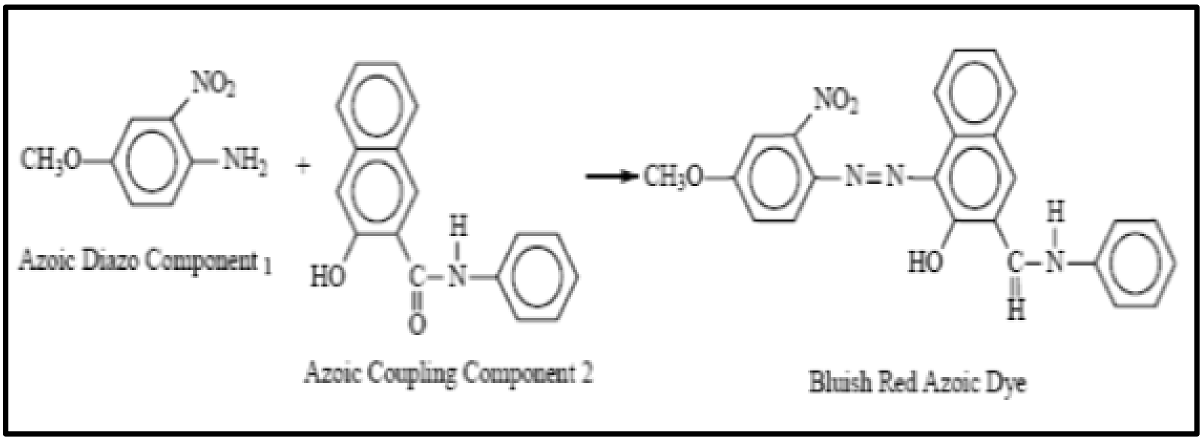

Fig. 1.1 Structure of Azo dyes. Adopted from the reference [5]

Anthraquinone dyes: These dyes are commonly used in the production of textiles, plastics, and printing inks. They are derived from Anthraquinone, a compound found in plants.

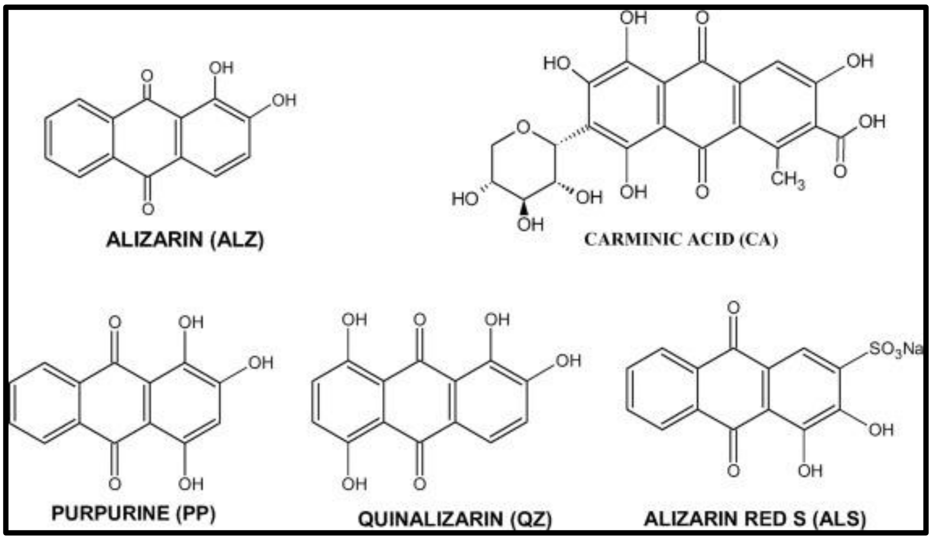

Fig. 1.2 Structure of Anthraquinone dyes. Adopted from the reference [6]

Phthalocyanine dyes: These dyes are used in the production of inks, coatings, and plastics. They are known for their bright blue and green colors and are often used in printing applications.

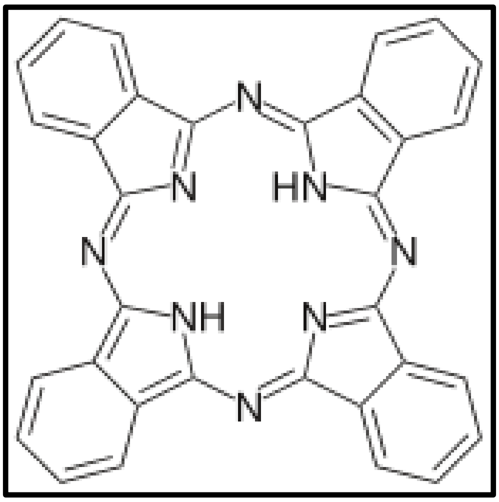

Fig. 1.3 Structure of Phthalocyanine dye. Adopted from the reference[7]

Triphenylmethane dyes: These dyes are commonly used in the production of paper, textiles, and leather. They are known for their bright and vivid colors, such as magenta and turquoise.

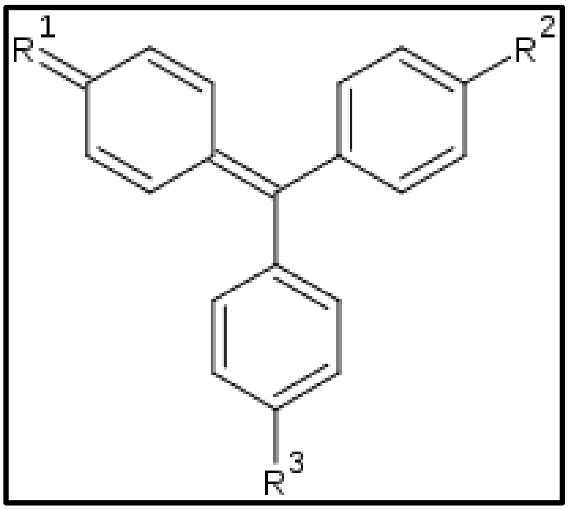

Fig. 1.4 Structure of Triphenylmethane dyes. Adopted from the reference[8]

Nitro dyes: These dyes are used in the production of dyes for cellulose fibers and are known for their bright and vibrant colors.

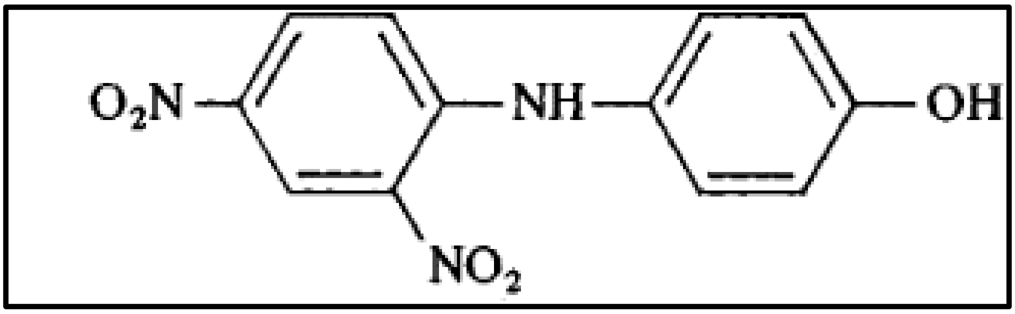

Fig.1.5 Structure of Nitro dyes. Adopted from the reference[9]

Natural dyes: These dyes are derived from natural sources such as plants, insects, and minerals. They are often used in the production of textiles and are considered to be more environmentally friendly than synthetic dyes.

Overall, there are many different types of organic dyes that are used in industries for various purposes, and each type of dye can have different environmental impacts if not properly managed and treated before discharge into water bodies.

1.3 Toxicity of dyes

When the release of dyes from various industries into the water bodies are not properly treated and disposed of, they can enter waterways and have negative impacts on aquatic ecosystems. In particular, some organic dyes can be toxic and hazardous to fish and other aquatic organisms, which can ultimately affect the entire food chain. In addition, exposure to certain organic dyes has been linked to increased risk of cancer and mutations in humans. This is because some organic dyes can interact with DNA and cause damage to cells, leading to genetic mutations and potentially cancerous growths.

Organic dyes can be toxic for various reasons, including their chemical structure, solubility, and persistence in the environment. One way that organic dyes can be toxic is through their chemical structure. Some dyes contain aromatic compounds or other chemical groups that can be harmful to living organisms. For example, some dyes contain azo compounds, which can break down into toxic aromatic amines that are known to be carcinogenic.

Also, Color blocks light penetration which delays photosynthetic activity and also has a tendency to chelate metal ions which result in micro-toxicity to fish and other organisms. The dyes undergo oxidation and reduction in water which produces toxic and hazardous intermediates/substances which further increase the need for their removal from wastewater[10]. The remnants of dyes in water pose a serious problem during the water purification process. The dyes are being designed with combination of complexes which when leach out in water do not get break down and mark their existence for a very long period of time which disturb the water ecosystem[4].

1.4Techniques for dye detection

Organic dyes can be detected using a variety of techniques, some of which include:

UV-Vis Spectroscopy: This technique involves measuring the absorption or transmission of ultraviolet and visible light by the dye molecule. Organic dyes tend to absorb light in the visible range, which can be used to identify and quantify the dye. [11]

Fluorescence Spectroscopy: Organic dyes can often emit fluorescent light when excited by a specific wavelength of light. Fluorescence spectroscopy measures this emission, which can be used to identify and quantify the dye. [12]

High-Performance Liquid Chromatography (HPLC): HPLC is a chromatographic technique that separates compounds based on their solubility and interaction with a stationary phase. Organic dyes can be separated and detected using HPLC, which can provide information about their identity and concentration. [13]

Mass Spectrometry: Mass spectrometry is a powerful analytical technique that can be used to identify and characterize organic dyes. This technique involves ionizing the sample and measuring the mass-to-charge ratio of the resulting ions.

Infrared Spectroscopy: Infrared spectroscopy involves measuring the absorption of infrared light by a molecule. Organic dyes have unique infrared spectra that can be used to identify and quantify them.

Even though the above mentioned techniques can be used to detect some dye, Detection of specific dyes in effluents is a great challenge. Although, dyes are highly colored molecules, their spectrophotometric detection is not possible due to interference of spectral lines in a mixture containing a number of dyes including, R6G, RhB, MB, , methyl orange (MO), methyl red (MR), acridine orange (AO), indigo carmine (IC), methyl violet (MV), etc. [14]

Hence, the direct determination of these dyes in wastewater effluents is laborious and cost-intensive and thus requires special techniques and procedures. Moreover, several dyes, particularly azo dyes, undergo photochemical or biological degradation in the aquatic environment.

1.5 Prevention

To mitigate the negative impacts of organic dyes in water bodies, some of the ways include:

Implementing proper waste management practices: The first step in preventing the negative impact of organic dyes on water bodies is to implement proper waste management practices. This includes treating the wastewater generated by dyeing processes before it is released into water bodies.

Use eco-friendly dyes: Companies should switch to eco-friendly dyes that are less harmful to the environment. These dyes are made from natural and biodegradable materials and are safer for water bodies.

Recycle water: Companies can recycle the water used in dyeing processes instead of releasing it into water bodies. This can be done by treating the wastewater and reusing it in the dyeing process.[11]

Conduct regular water quality tests: Companies should conduct regular water quality tests to ensure that the water being discharged from their facilities meets regulatory standards. If the water quality is found to be below standard, corrective action should be taken immediately.

Implement a sustainable manufacturing process: Companies should implement a sustainable manufacturing process that takes into account the impact of their operations on the environment. This includes reducing water usage, energy consumption, and waste generation.

Overall, preventing the negative impact of organic dyes on water bodies requires a combination of proper waste management practices, the use of eco-friendly dyes, and a sustainable manufacturing process. By implementing these measures, companies can minimize their impact on the environment and protect water bodies from harmful pollutants. It is important to properly treat and dispose of dye waste, and to use alternative, non-toxic dyes when possible. In addition, regulatory agencies may impose restrictions on the use of certain organic dyes in order to protect human health and the environment.[15]

1.6 Lead based Perovskites

Lead-based perovskites have shown promise in the field of environmental remediation, particularly in treating organic pollutants in water. Perovskite materials are a class of materials that have a unique crystal structure based on the composition ABX3, where A and B are cations and X is an anion. [16] Lead-based perovskites, in particular, have attracted significant attention due to their exceptional optical and electronic properties, which make them ideal for use in solar cells and other energy applications.

In recent years, researchers have also been exploring the use of lead-based perovskites for environmental remediation applications, such as the treatment of organic pollutants in water. Lead-based perovskites have been shown to effectively remove various organic pollutants, including dyes, pesticides, and pharmaceuticals, from water through a process called photocatalysis. During photocatalysis, the perovskite material absorbs light energy and uses it to generate reactive oxygen species that can degrade and break down organic pollutants in the water.[17] have shown that lead-based perovskites can effectively degrade a range of organic pollutants, including dyes and pharmaceuticals. However, the use of lead in these materials has raised concerns about potential environmental and health risks.

Overall, the use of lead-based perovskites for treating organic pollutants is a promising area of research that could potentially offer a more sustainable and effective solution for water pollution. However, it is important to carefully consider the potential risks and benefits before implementing these materials on a large scale.

Lead is a highly toxic heavy metal that can cause serious health problems in humans and wildlife. Exposure to lead can occur through ingestion, inhalation, or skin contact with lead-containing materials or contaminated soil and water. [18]

Lead toxicity can have a range of negative effects on the body, including damage to the nervous system, kidneys, and reproductive system. Children and pregnant women are particularly vulnerable to the harmful effects of lead, which can lead to developmental delays and neurological problems.[19]

In the context of treating organic pollutants, the use of lead-based materials such as lead-based perovskites raises concerns about potential environmental and health risks. While lead-based perovskites have shown promise for degrading organic pollutants in water, the potential risks associated with lead exposure must be carefully considered.

To minimize the potential risks of lead toxicity, it is important to implement safe handling and disposal practices for lead-containing materials. This includes following proper safety protocols when working with lead-based perovskites or other lead-containing materials, such as wearing protective equipment and properly disposing of waste materials. It is also important to explore alternative materials that do not contain lead, such as lead-free perovskites, to minimize the potential risks associated with lead toxicity. By carefully considering the potential risks and benefits of different materials and implementing safe handling and disposal practices, it may be possible to effectively treat organic pollutants without posing undue risks to human health or the environment.

1.7 Lead free halide perovskites

Halide perovskites are a class of materials that have been receiving a lot of attention in recent years due to their exceptional optoelectronic properties. They are a type of perovskite crystal structure composed of a metal halide framework (such as lead, tin, or cesium) and an organic cation (such as methylammonium (MA) or formamidinium (FA)). The most commonly studied halide perovskites are based on lead, such as methylammonium lead iodide ($MAPbI_3$) or formamidinium lead iodide ($FAPbI_3$). [19]

These materials have emerged as promising candidates for a range of optoelectronic applications, including solar cells, light-emitting diodes (LEDs), and photodetectors. They have high carrier mobility and long carrier lifetimes, which result in high photovoltaic efficiency. Halide perovskites have also demonstrated remarkable color purity and brightness in LEDs.[20]

One of the most promising applications of halide perovskites in photocatalysis is in the area of water splitting, which involves the use of sunlight to split water into hydrogen and oxygen. Halide perovskites have been shown to be effective photocatalysts for this reaction, with some studies reporting impressive hydrogen evolution rates.

Another area where halide perovskites have shown promise is in the degradation of organic pollutants. Researchers have shown that these materials can be used to efficiently break down pollutants such as dyes and pharmaceuticals, which are often difficult to remove from wastewater using conventional treatment methods.

Halide perovskites have a unique combination of properties, including high light absorption coefficients, wide light absorption ranges, tunable band gaps, and long carrier lifetimes.

Their high light absorption coefficients arise from their ability to absorb light across a broad spectrum, including both visible and infrared light. This is due to their high charge carrier mobilities and long carrier lifetimes, which allow them to efficiently capture and transport light-generated carriers.

The tunable band gap of halide perovskites is a particularly useful property for solar cells because it allows for the material's absorption range to be tailored to specific solar cell applications. By controlling the composition and crystal structure of the perovskite, the band gap can be adjusted, which enables these materials to capture light in a wider range of the solar spectrum.

Furthermore, halide perovskites have shown long carrier lifetimes, which means that the carriers generated by absorbed light can persist in the material for an extended period. This is an essential property for efficient charge transport, which is critical for achieving high power conversion efficiencies in solar cells. Overall, the unique properties of halide perovskites make them attractive candidates for a wide range of photocatalytic applications, and research in this area is likely to continue to grow in the coming years. However, there are also some challenges that need to be addressed, such as the stability of these materials under photocatalytic conditions, which will require further investigation. Highly-efficient and stable photocatalytic activity of lead-free $Cs_2AgInCl_6$ double perovskite for organic pollutant degradation.[21]

1.8 $Cs_2AgInCl_6$

The double perovskites (DP), $A_2B(I)B(II)X_6$ is a type of perovskite structure that can be formed by replacing two divalent Pb^{2+} ions in the crystal lattice with metal cations of the monovalent B^+ and trivalent B^{3+}.

Theoretical calculations have shown that DPs have excellent stability and non-toxicity compared to lead-based perovskites. This makes them promising candidates for use in solar cells and other optoelectronic devices.

Furthermore, DPs have shown promise for their tunable electronic properties and potential for enhanced stability in ambient conditions. However, more research is needed to fully understand their properties and potential applications.[16] Highly-efficient and stable photocatalytic activity of lead-free $Cs_2AgInCl_6$ double perovskite for organic pollutant degradation

$Cs_2AgInCl_6$ has been reported to exhibit good stability against thermal and light conditions.$Cs_2AgInCl_6$ is a type of inorganic compound that belongs to the family of double perovskite materials. $Cs_2AgInCl_6$ is a promising material for photocatalytic applications due to its direct band gap and long carrier lifetime. A direct band gap material is one where the energy difference between the valence band and the conduction band is such that an electron can directly transition from the valence band to the conduction band, resulting in the emission of a photon. This property makes $Cs_2AgInCl_6$ an efficient absorber of light, particularly in the visible range.

In addition to its direct band gap,$Cs_2AgInCl_6$ also has a long carrier lifetime, which means that the electrons and holes generated by the absorption of light persist in the material for a relatively long time before recombining. This property is essential for photocatalytic applications, as it allows the electrons and holes to participate in chemical reactions before they recombine. Therefore, $Cs_2AgInCl_6$'s unique properties make it a promising candidate for photocatalytic applications, including water splitting and CO_2 reduction. By using $Cs_2AgInCl_6$ as a photocatalyst, it may be possible to produce clean and sustainable fuels, such as hydrogen, using sunlight as the energy source.[21]

2. Experimental section

2.1 Materials

Hydrochloric Acid (HCl, 37 wt%), Cesium Chloride (CsCl, 99.9%), Indium (III) Chloride (InCl3, 99.9%) Silver Chloride (AgCl, 99.9%), Methyl orange (MO) and Sudan Red III were purchased from Alfa Aesar and Sigma Aldrich. All the precursors are used as received without any further purification.

Fig. 2.1: Chemicals used for preparation of compounds

2.2 Synthesis

The series $Cs_2AgIn_{(1-x)}Sb_xCl_6$ was prepared using precipitation method using the following reactants, CsCl, AgCl, $InCl_3$ and $SbCl_3$ in stoichiometric ratios. The reactants undergo the following chemical reaction in 37% HCl which was used as the solvent to facilitate the reaction.

The following reaction takes place.

$$2CsCl + AgCl + InCl_3 + SbCl_3 \xrightarrow{\text{In HCl at } 75^oC} Cs_2AgIn_{(1-x)}Sb_xCl_6$$

Stoichiometric ratios of AgCl, $InCl_3$, $SbCl_3$ were taken in about 10 ml HCl and stirred continuously while heating. The mixture was heated at 75^oC for thirty minutes before adding calculated amount of CsCl. As soon as CsCl was added to the mixture a yellowish precipitate was formed. This was further stirred for thirty minutes. The contents were then filtered and collected in a beaker and washed in ethanol four times to remove any HCl. The precipitate was then dried in ethanol overnight at 90^oC and the powdered sample was ground and collected for characterization and other studies. All the samples were yellowish white in colour with varying degrees of yellow tinge. Figure 2.2 below depicts the schematics of the above reaction.

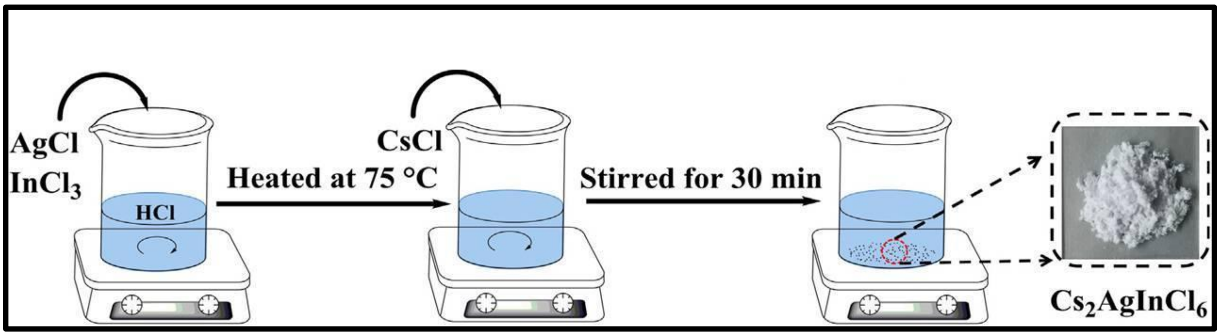

Fig. 2.2 Schematic diagrams of the synthesis process of $Cs_2AgInCl_6$

Adopted from the reference [21]

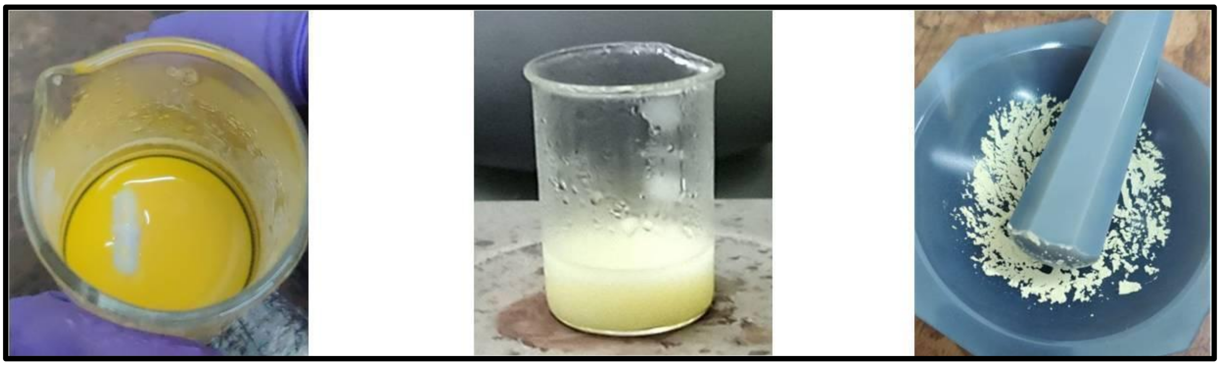

Fig. 2.3 Preparation of the compound $Cs_2AgInCl_6$

3. Characterization

Characterization, refers to the broad and general process by which a material's structure and properties are probed and measured. It is a fundamental process in the field of materials science, without which no scientific understanding of engineering materials could be ascertained.

Characterization is very important for development of good quality materials. The complete characterization of any material consists of phase analysis, structural and compositional characterization, micro-structural analysis and spectroscopic analysis. One single technique is not capable of providing complete characterization of a solid. In this chapter different analytical instrumental techniques are discussed which were used to characterize the samples prepared.

3.1 X-ray Diffraction

X-ray powder diffraction (XRD) is a rapid analytical technique primarily used for phase identification of a crystalline material and can provide information on unit cell dimensions. The analyzed material is finely ground, homogenized, and average bulk composition is determined.[18]

3.1.1 Generation of X-rays

X-rays are electromagnetic radiation having wavelength ~1Å. X-rays are produced when high energy particles such as electrons are accelerated through high potential to collide with target material. The resulting X-ray spectra usually have two components: a broad spectrum of wavelengths known as white radiation and a number of fixed or monochromatic wavelengths. X-rays which are used in X-ray diffractometers are monochromatic X-rays. A beam of electrons when accelerated through high potential differences are allowed to strike a metal target such as Cu. The incident electron beam has sufficient energy to ionize some of the Cu K shell electrons. An electron in the outer orbit (such as L, M) can fill the vacancy created in the K shell and the energy released in the transition appears as X-radiation. For Cu, transition from L-shell to K-shell appears as Kα radiation and transition from M-shell to K-shell appears as Kβ radiation.

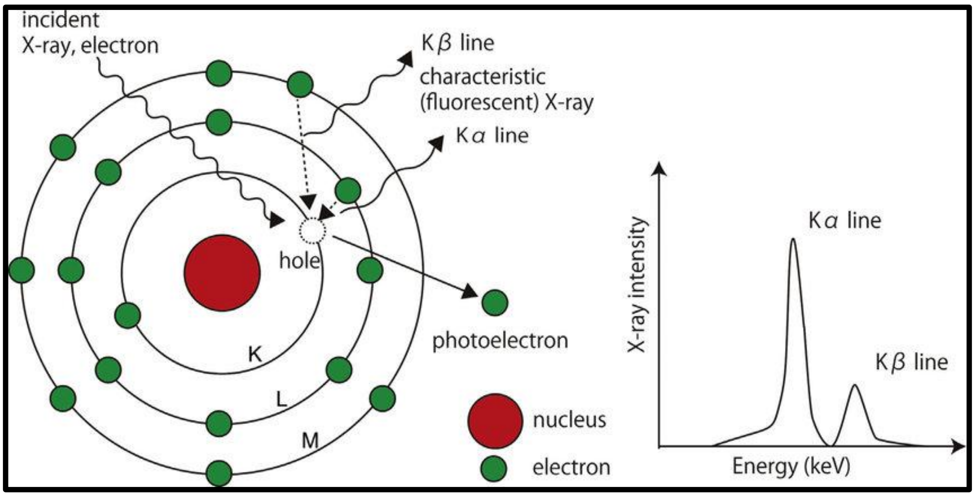

Fig. 3.1: a) Generation of Cu Kα X-rays, b) X-ray emission spectrum of Cu

Adopted from the reference[22]

3.1.2 Interaction of X-rays with matter

Bragg's approach to diffraction is to regard the crystals as built up in layers or planes and each plane acts as a semi-transparent mirror. When X-rays with wavelength similar to atomic spacings are incident upon a crystalline material, some of the x-rays are reflected off the plane with an incidence equal to angle of reflection and the rest are transmitted to be subsequently reflected by succeeding planes.

Bragg's Law

$$2d\ Sin\theta = n\lambda \ldots\ldots\ldots\ldots\ldots\ldots\ldots\ldots\ldots\ldots\ldots\ldots\ldots\ldots\ldots (3.1)$$

Where;

d is interplanar spacing, θ is Bragg's angle of diffraction angle, λ is Wavelength of X-rays used and n is order of diffraction. [2]

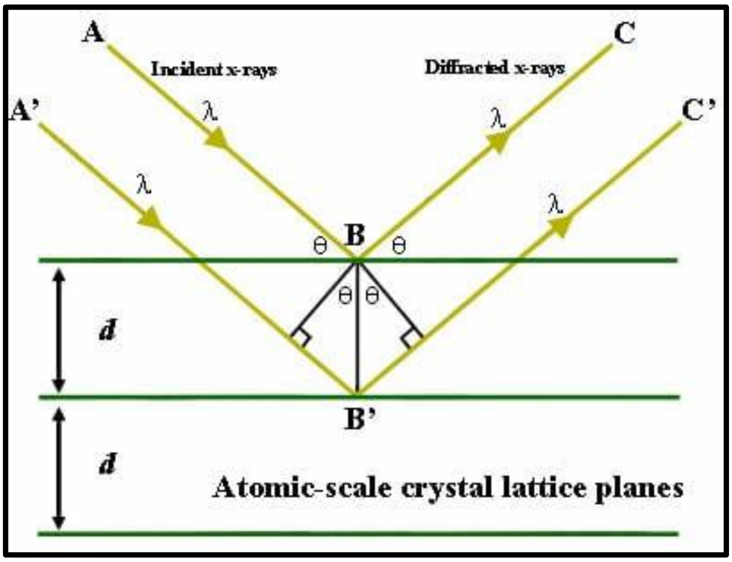

Fig. 3.2: Schematic representation of Bragg's Law. Adopted from the reference [23]

When Bragg's law is satisfied, the reflected beams are in phase and they interfere constructively. For angles other than Bragg's angle, they are out of phase and interfere destructively. Bragg's law imposes a strict condition on the angles at which reflection may occur.

3.1.3 Powder XRD method

In this method, a monochromatic beam of x-rays strikes a finely powdered sample in which there is random orientation of crystals in every possible direction. In such powdered samples, various planes are also present in every possible orientation. For each set of planes, at least some crystals must be oriented in at Bragg's angle, to the incident beam and thus Bragg's law is satisfied for those crystals and planes. The diffracted beam is then detected by the detector. For any set of lattice planes, the diffracted radiation from the surface of a cone. The only requirement for diffraction is that the planes should be at Bragg's angle with respect to the incident beam and no restriction is placed on the angular orientation of the planes about the axis of the incident beam. In a finely powdered sample, crystals are present at every possible angular position about the incident beam so the diffracted radiation appears to be emitted from the sample as cones of radiation. Each set of planes gives its own cone of radiation.

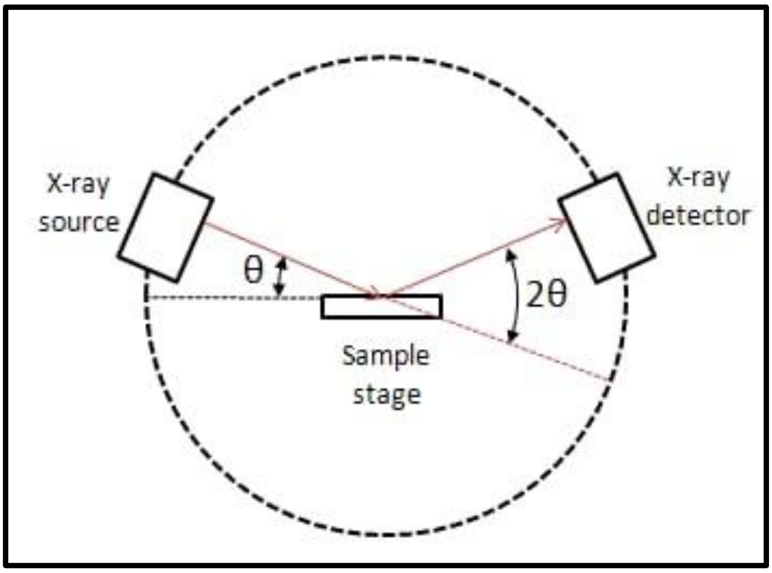

Fig. 3.3 Formation of the cone of a diffracted beam. Adopted from reference [24]

3.1.4 Powder X-ray Diffractometer

Powder X-ray Diffractometer consists of following components:

<u>X-ray Source</u>: High energy electrons are produced from heated tungsten filament and this is allowed to impinge on small metal target example Copper in a sealed diffraction tube.

Collimator: X-rays are generated by target material and then it passes through the collimator. It consists of a set of two metal plates which are closely packed and separated by a small distance. The collimator absorbs all the x-rays except the narrow beam that passes through it.

Monochromators: Monochromators separate polychromatic light into a range of individual wavelengths. Graphite Monochromator is used in Rigaku SmartLab X-ray diffractometer. The graphite monochromator optimizes sensitivity by lowering the background level. It improves signal-to-noise by eliminating fluorescence from Co, Ni, Fe, Mn containing materials.

Filters: Filters absorb undesirable radiations but allow the radiation of desired wavelength to pass. Example nickel filter is used to remove Kβ radiations of copper. These filters are used as an alternative to monochromators.

Detector: The D/TEX Ultra 250 is used to detect the diffracted beam in Rigaku Smart lab powder X-ray diffractometer. It is a 1D Silicon strip detector that decreases data acquisition time by 50% compared to competitive detectors. This is achieved by increasing the active area of the aperture and thus increasing the count rate. D/TEX ultra has smaller pixel pitch and longer in direction of 2θ. [Rigaku smart lab x-ray diffractometer.

3.1.5 Applications

X-ray powder diffraction is most widely used for the identification of unknown crystalline materials (e.g. minerals, inorganic compounds). Determination of unknown solids is critical to studies in geology, environmental science, material science, engineering and biology.

Other applications include:

- characterization of crystalline materials
- identification of fine-grained minerals such as clays and mixed layer clays that are difficult to determine optically
- determination of unit cell dimensions
- measurement of sample purity

With specialized techniques, XRD can be used to:

- determine crystal structures using Rietveld refinement
- determine of modal amounts of minerals (quantitative analysis)
- characterize thin films samples by:
    - determining lattice mismatch between film and substrate and to inferring stress and strain
    - determining dislocation density and quality of the film by rocking curve measurements
    - measuring superlattices in multilayered epitaxial structures
    - determining the thickness, roughness and density of the film using glancing incidence X-ray reflectivity measurements
- make textural measurements, such as the orientation of grains, in a polycrystalline sample.

3.1.6 Strengths and Limitations of X-ray Powder Diffraction (XRD)

Strengths

- Powerful and rapid (< 20 min) technique for identification of an unknown mineral

- In most cases, it provides an unambiguous mineral determination
- Minimal sample preparation is required
- XRD units are widely available
- Data interpretation is relatively straight forward

Limitations

- Homogeneous and single phase material is best for identification of an unknown
- Must have access to a standard reference file of inorganic compounds (d-spacings, *hkl'*s)
- Requires tenths of a gram of material which must be ground into a powder
- For mixed materials, detection limit is ~ 2% of sample
- For unit cell determinations, indexing of patterns for non-isometric crystal systems is complicated
- Peak overlay may occur and worsens for high angle 'reflections'[25,26,27,28]

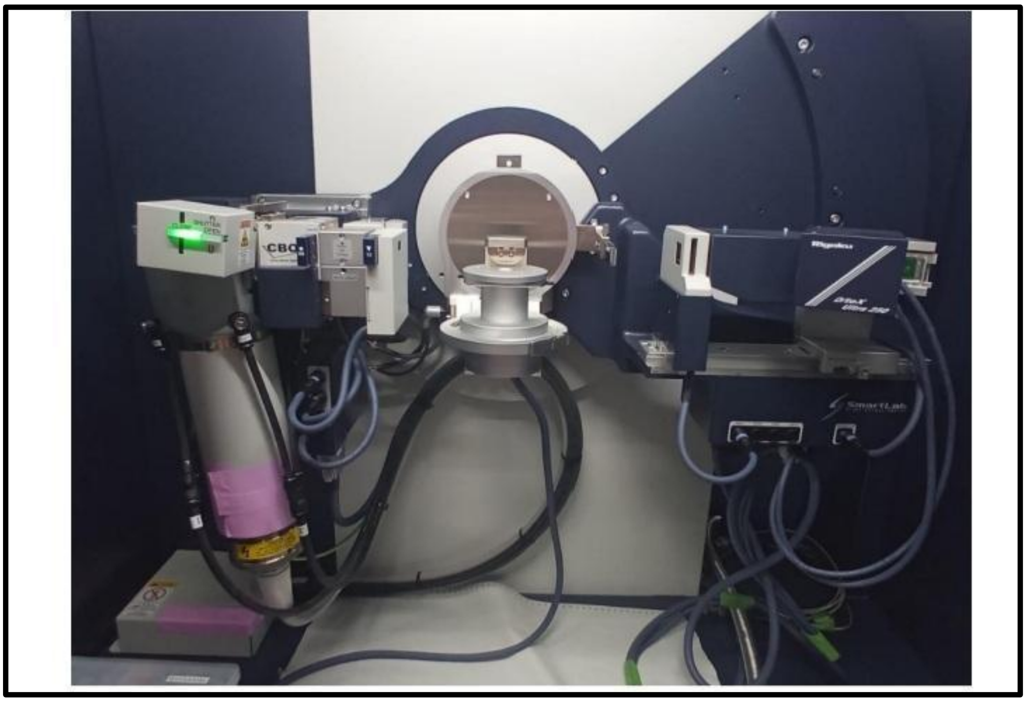

Fig. 3.4: Rigaku Smart Lab Powder X-ray diffractometer at ULMC of Goa University.

3.2 UV-Vis Spectroscopy

3.2.1 What is UV-Vis spectroscopy?

UV-Vis spectroscopy is an analytical technique that measures the amount of discrete wavelengths of UV or visible light that are absorbed by or transmitted through a sample in comparison to a reference or blank sample. This property is influenced by the sample composition, potentially providing information on what is in the sample and at what concentration. Since this spectroscopy technique relies on the use of light, let's first consider the properties of light.

Light has a certain amount of energy which is inversely proportional to its wavelength. Thus, shorter wavelengths of light carry more energy and longer wavelengths carry less energy. A specific amount of energy is needed to promote electrons in a substance to a higher energy state which we can detect as absorption. Electrons in different bonding environments in a substance require a different specific amount of energy to promote the electrons to a higher energy state. This is why the absorption of light occurs for different wavelengths in different substances. Humans are able to see a spectrum of visible light, from approximately 380 nm, which we see as violet, to 780 nm, which we see as red.1 UV light has wavelengths shorter than that of visible light to approximately 100 nm. Therefore, light can be described by its wavelength, which can be useful in UV-Vis spectroscopy to analyze or identify different substances by locating the specific wavelengths corresponding to maximum absorbance (see the Applications of UV-Vis spectroscopy section). [29]

3.2.2 Principle

A compound appears coloured if it selectively absorbs light from the visible region. The absorbed energy raises the molecule from ground energy state (E0) to higher excited energy state (E1).

$$\Delta E = E1 - E0 = h\nu = hc/\lambda \ldots\ldots\ldots\ldots\ldots\ldots\ldots\ldots(3.2)$$

The difference in energy ΔE depends on how tightly the electrons are bound to the bonds, and accordingly absorption will occur in UV or visible range. In compounds having sigma bonds, the electrons in the molecule are tightly bound so radiation from the UV region will be absorbed. No absorption occurs in the visible region, so the compound appears colourless. If the electrons in the molecule are loosely bound, absorption occurs in the visible region and the compound appears coloured.

There are three types of ground state orbitals in molecules:

a) σ (bonding) molecular orbital – Electrons in this orbital are tightly bound and require high energy for their excitation and thus do not show absorption near the UV region.

b) π (bonding) molecular orbital – Electrons in this orbital are found in multiple bonds and are generally mobile. Since π bonds are weak, the energy produced by UV radiation can excite its electrons from ground level to higher energy levels.

c) n (non-bonding) molecular orbital – Valence electrons which do not participate to form a chemical bond in a molecule are called non-bonding electrons or n electrons. These are generally lone pairs of electrons and can be excited by UV radiation.

Besides these, the anti-bonding orbitals are σ* orbital and π* orbital. [UV-Vis spectroscopy]

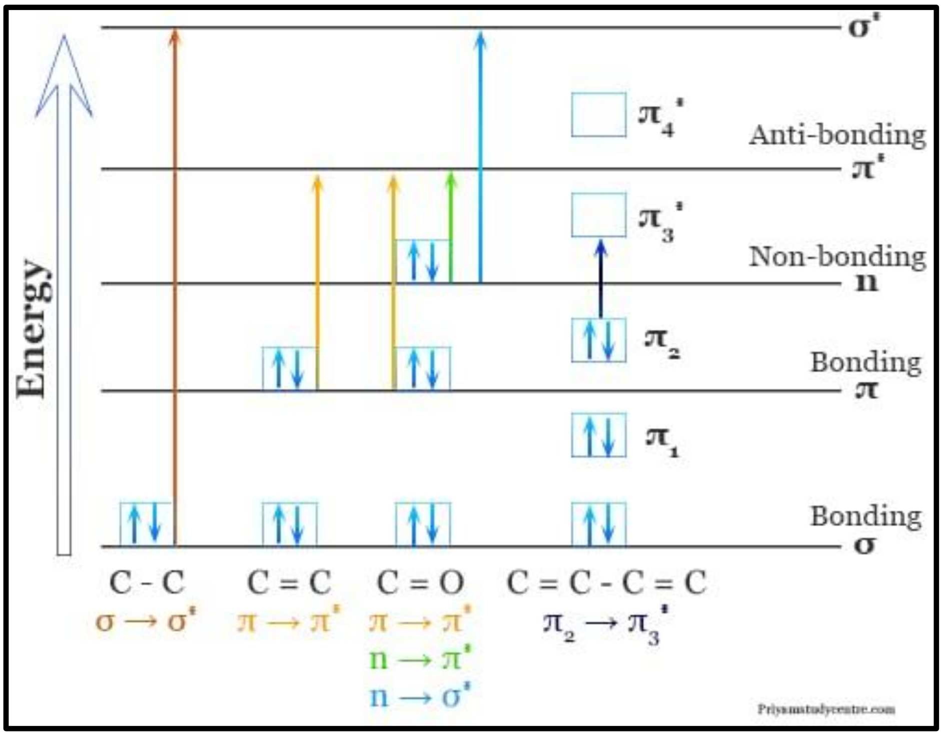

Fig. 3.5 Electronic transitions in UV-Visible spectroscopy. Adopted from the reference [30]

3.2.3 Beer-Lambert Law

A light beam is emitted via source and the incident beam passes through the sample and the wavelength of light reaching the detector is measured. The measured wavelength provides qualitative and quantitative information about the loaded sample such as chemical structure and number of molecules present. The information can be obtained as absorbance, transmittance or reflectance of radiation of range 160 nm to 3500 nm. When a light beam of specific energy (intensity) is focused onto a sample, the molecules absorb some energy of the incident light. A photodetector measures the intensity of light coming out of the sample and registers its absorbance. The absorption or transmission spectra of the light absorbed or transmitted by the sample against the wavelength is recorded. Beer-Lambert Law is the basic principle of quantitative analysis which states that absorbance of light by the sample is directly proportional to analyte concentration and optical path length.

$$A = \varepsilon.\, l.\, c \;\ldots\ldots\ldots\ldots\ldots\ldots\ldots(\,3.3)$$

Where ε is molar absorption coefficient, l is optical path length and c is molar concentration. Transmittance (T) is given by

$$T = I/Io \;\ldots\ldots\ldots\ldots\ldots\ldots\ldots\ldots\ldots(\,3.4)$$

Where I is intensity of incident light and Io is the intensity of light detected and absorbance is the inverse of transmittance given by

$$A = \log\,(\,1\;T\,) = \log\,(\,I\;Io) = -\varepsilon c l \;\ldots\ldots\ldots\ldots\ldots\ldots(3.5)$$

3.2.4 Instrumentation

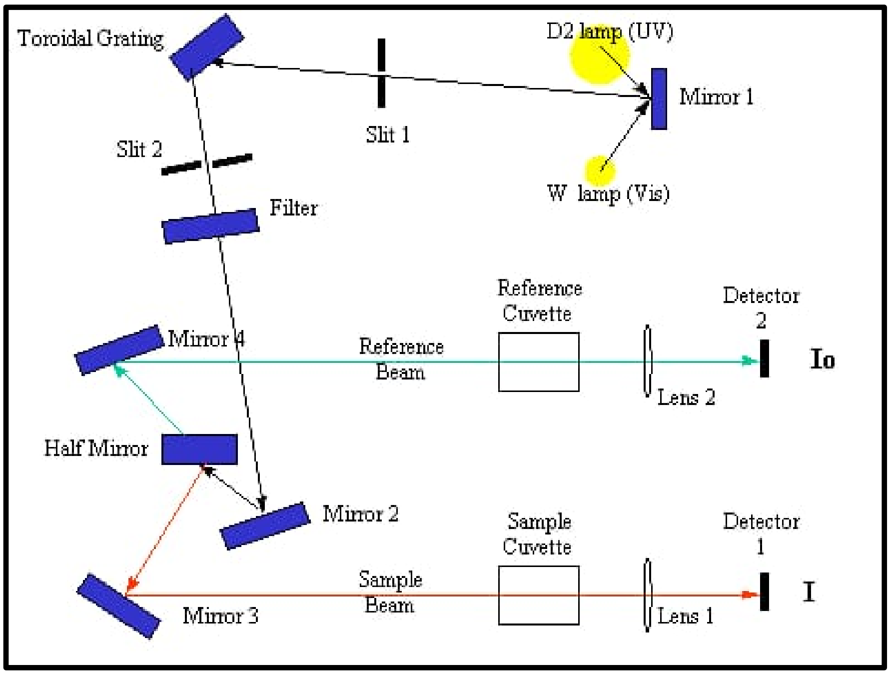

Fig. 3.6 : Schematic representation of UV- Visible Spectrometer.

Adopted from the reference [31]

The instrument consists of a UV source which produces continuous UV spectrum by electrically exciting deuterium or hydrogen at low pressures, a visible light source which is generally a Tungsten filament lamp, a monochromator and before reaching the sample, the light is divided into two parts of similar intensity with a half mirror splitter. One part travels via a cuvette having a solution of material to be examined in a transparent solvent and the second beam or reference beam travels through a cuvette having only solvent.

The detector detects the intensity of light transmitted by both the cuvettes and sends that data to a meter to record and display the values. Electronic detectors calculate and compare the intensities of the light beams. [34]

3.2.5 How does a UV-Vis spectrophotometer work?

Whilst there are many variations on the UV-Vis spectrophotometer, to gain a better understanding of how an UV-Vis spectrophotometer works, let us consider the main components, depicted in Figure 3.7. A simplified schematic of the main components in a UV-Vis spectrophotometer. The path of light from the light source, to the wavelength selector, sample and detector prior to signal processing is shown.

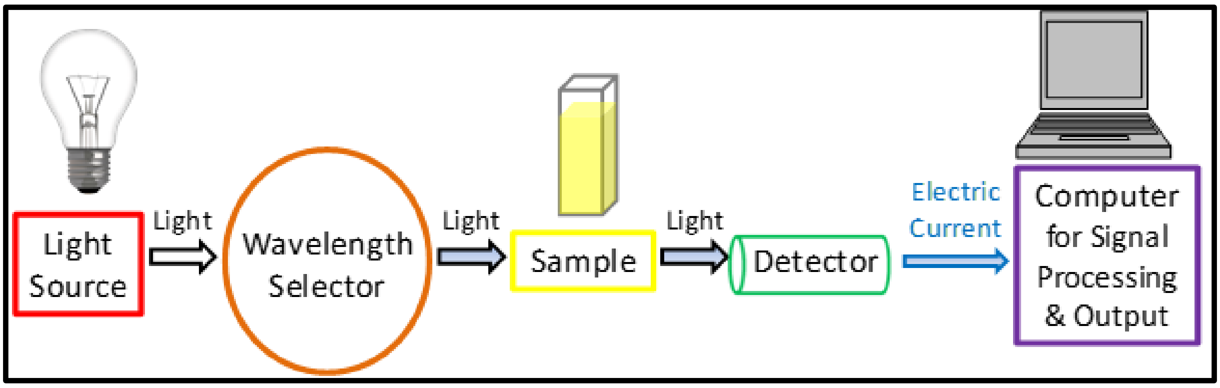

Fig. 3.7: A simplified schematic of the main components in a UV-Vis spectrophotometer. Adopted from the reference [32]

Light source: As a light-based technique, a steady source able to emit light across a wide range of wavelengths is essential. A single xenon lamp is commonly used as a high intensity light source for both UV and visible ranges. Xenon lamps are, however, associated with higher costs and are less stable in comparison to tungsten and halogen lamps.

For instruments employing two lamps, a tungsten or halogen lamp is commonly used for visible light, whilst a deuterium lamp is the common source of UV light. As two different light sources are needed to scan both the UV and visible wavelengths, the light source in the instrument must switch during measurement. In practice, this switchover typically occurs during the scan between 300 and 350 nm where the light emission is similar from both light sources and the transition can be made more smoothly.

Wavelength selection: In the next step, certain wavelengths of light suited to the sample type and analyte for detection must be selected for sample examination from the broad wavelengths emitted by the light source. Available methods for this include:

Monochromators - A monochromator separates light into a narrow band of wavelengths. It is most often based on diffraction gratings that can be rotated to choose incoming and reflected angles to select the desired wavelength of light. The diffraction grating's groove frequency is often measured as the number of grooves per mm. A higher groove frequency provides a better optical resolution but a narrower usable wavelength range. A lower groove frequency provides a larger usable wavelength range but a worse optical resolution. 300 to 2000 grooves per mm is usable for UV-Vis spectroscopy purposes but a minimum of 1200 grooves per mm is typical. The quality of the spectroscopic measurements is sensitive to physical imperfections in the diffraction grating and in the optical setup. As a consequence, ruled diffraction gratings tend to have more defects than blazed holographic diffraction gratings.Blazed holographic diffraction gratings tend to provide significantly better quality measurements.

Absorption filters - Absorption filters are commonly made of colored glass or plastic designed to absorb particular wavelengths of light.

Interference filters - Also called dichroic filters, these commonly used filters are made of many layers of dielectric material where interference occurs between the thin layers of materials. These filters can be used to eliminate undesirable wavelengths by destructive interference, thus acting as a wavelength selector.

Cutoff filters - Cutoff filters allow light either below (shortpass) or above (longpass) a certain wavelength to pass through. These are commonly implemented using interference filters.

Bandpass filters -Bandpass filters allow a range of wavelengths to pass through that can be implemented by combining shortpass and longpass filters together.

Monochromators are most commonly used for this process due to their versatility. However, filters are often used together with monochromators to narrow the wavelengths of light selected further for more precise measurements and to improve the signal-to-noise ratio.

Sample analysis: Whichever wavelength selector is used in the spectrophotometer, the light then passes through a sample. For all analyses, measuring a reference sample, often referred to as the "blank sample", such as a cuvette filled with a similar solvent used to prepare the sample, is imperative. If an aqueous buffered solution containing the sample is used for measurements, then the aqueous buffered solution without the substance of interest is used as the reference. When examining bacterial cultures, the sterile culture media would be used as the reference. The reference sample signal is then later used automatically by the instrument to help obtain the true absorbance values of the analytes.

It is important to be aware of the materials and conditions used in UV-Vis spectroscopy experiments. For example, the majority of plastic cuvettes are inappropriate for UV absorption studies because plastic generally absorbs UV light. Glass can act as a filter, often absorbing the majority of UVC (100-280 nm)2 and UVB (280-315 nm)2 but allowing some UVA (315-400 nm)2 to pass through. Therefore, quartz sample holders are required for UV examination because quartz is transparent to the majority of UV light. Air may also be thought of as a filter because wavelengths of light shorter than about 200 nm are absorbed by molecular oxygen in the air. A special and more expensive setup is required for measurements with wavelengths shorter than 200 nm, usually involving an optical system filled with pure argon gas. Cuvette-free systems are also available that enable the analysis of very small sample volumes, for example in DNA or RNA analyses.

Detection: After the light has passed through the sample, a detector is used to convert the light into a readable electronic signal. Generally, detectors are based on photoelectric coatings or semiconductors.

A photoelectric coating ejects negatively charged electrons when exposed to light. When electrons are ejected, an electric current proportional to the light intensity is generated. A photomultiplier tube (PMT) is one of the more common detectors used in UV-Vis spectroscopy. A PMT is based on the photoelectric effect to initially eject electrons upon exposure to light, followed by sequential multiplication of the ejected electrons to generate a larger electric current.4 PMT detectors are especially useful for detecting very low levels of light. When semiconductors are exposed to light, an electric current proportional to the light intensity can pass through. More specifically, photodiodes6 and charge-coupled devices (CCDs) are two of the most common detectors based on semiconductor technology.

After the electric current is generated from whichever detector was used, the signal is then recognized and output to a computer or screen. Figures 3.8 and 3.9 show some simplified example schematic diagrams of UV-Vis spectrophotometer arrangements.

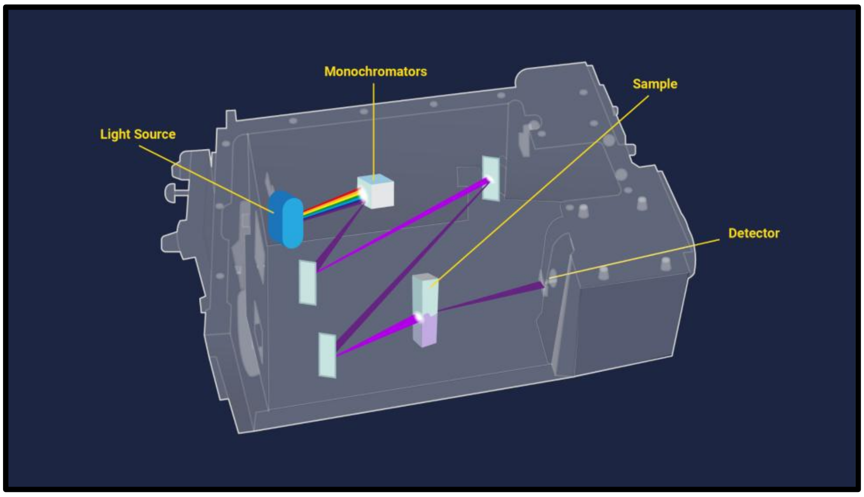

Fig. 3.8: Schematic diagram of a cuvette-based UV-Vis spectroscopy system.

Adopted from the reference [32]

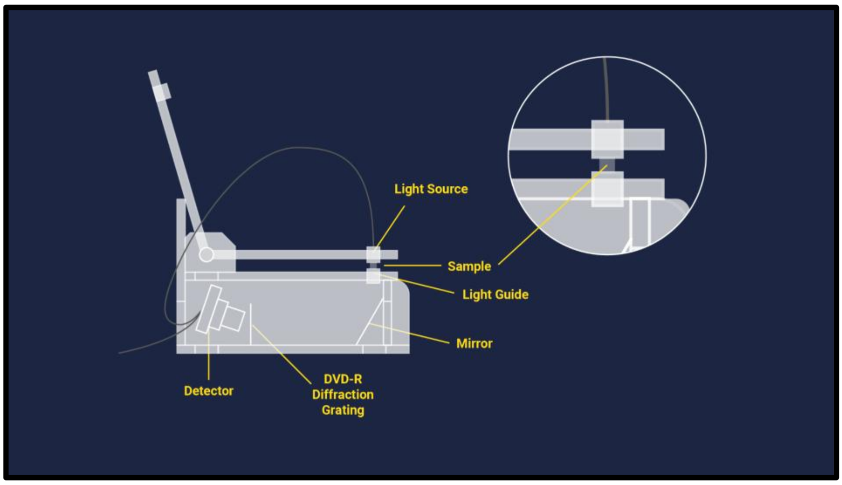

Fig. 3.9 : Schematic diagram of a cuvette-free UV-Vis spectroscopy system.

Adopted from the reference [32]

UV-Vis spectroscopy analysis, absorption spectrum and absorbance units

UV-Vis spectroscopy information may be presented as a graph of absorbance, optical density or transmittance as a function of wavelength. However, the information is more often presented as a graph of absorbance on the vertical y axis and wavelength on the horizontal x axis. This graph is typically referred to as an absorption spectrum; an example is shown in Figure 3.10.

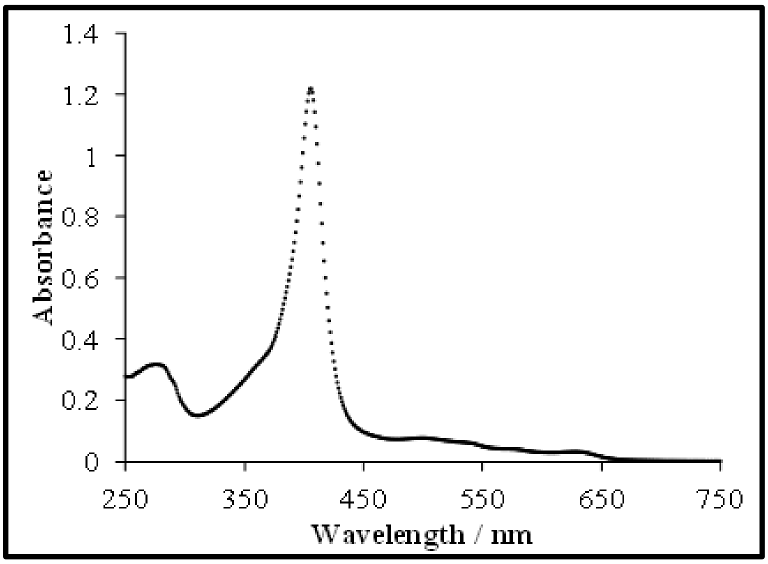

Fig. 3.10: An example absorption spectrum taken from a UV-Vis spectrophotometer.

Adopted from the reference [32]

Based on the UV-Vis spectrophotometer instrumentation reviewed in the previous section of this article, the intensity of light can be reasonably expected to be quantitatively related to the amount of light absorbed by the sample.

The absorbance (A) is equal to the logarithm of a fraction involving the intensity of light before passing through the sample (Io) divided by the intensity of light after passing through the sample (I). The fraction I divided by Io is also called transmittance (T), which expresses how much light has passed through a sample. However, Beer–Lambert's law is often applied to obtain the concentration of the sample (c) after measuring the absorbance (A) when the molar absorptivity (ε) and the path length (L) are known. Typically, ε is expressed with units of L mol-1 cm-1, L has units of cm, and c is expressed with units of mol L-1. As a consequence, A has no units. Sometimes AU is used to indicate arbitrary units or absorbance units but this has been strongly discouraged.

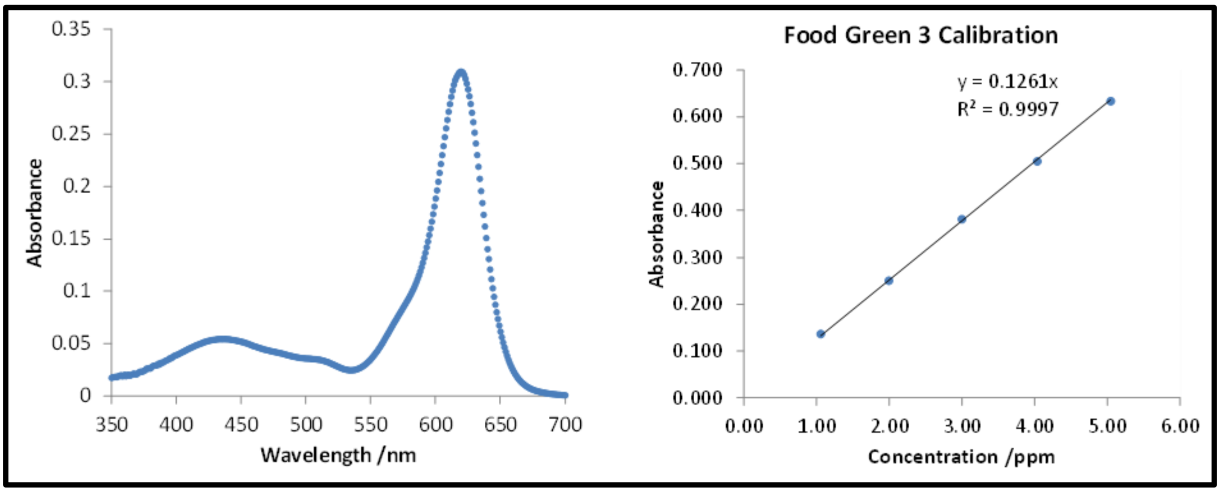

Fig. 3.11: A UV-Vis spectrum of Food Green 3 extracted from a sample is shown on the left graph. Adopted from the reference [32]

For data analysis, the graph of absorbance versus concentration can indicate how sensitive the system is when building a calibration curve. When a linear least squares regression equation is used, the slope from the line of best fit indicates sensitivity. If the slope is steeper, the sensitivity is higher. Sensitivity is the ability to differentiate between the small differences in the sample concentration. From Beer–Lambert's Law, the sensitivity can be partially indicated by the molar absorptivity ε. Knowing the ε values beforehand, if available, can help to determine the concentrations of the samples required, particularly where samples are limited or expensive.

For reliability and best practice, UV-Vis spectroscopy experiments and readings should be repeated. When repeating the examination of a sample, in general, a minimum of three replicate trials is common, but many more replicates are required in certain fields of work. A calculated quantity, such as the concentration of an unknown sample, is usually reported as an average with a standard deviation. Reproducible results are essential to ensure precise, high quality measurements. Standard deviation, relative standard deviation, or the coefficient of variation help to determine how precise the system and measurements are. A low deviation or variation indicates a higher level of precision and reliability.

3.2.6 Calculation of band gap from Diffuse reflectance Spectroscopy

Band gap energy is the energy needed to excite an electron from the valence band to the conduction band. Band gap energy is crucial in predicting photophysical and photochemical properties of some materials. In 1966, Tauc proposed a method to determine the band gap energy of materials using optical absorption spectra.

Tauc method is based on assumption that the energy-dependent absorption coefficient α can be expressed as

$$(\alpha .\, h\upsilon)^{1/\gamma} = \mathrm{B}(h\upsilon - E_g) \;\ldots\ldots\ldots\ldots(3.6)$$

Where h is Plank constant, υ is frequency of photon, Eg is band gap energy and B is constant. γ depends on the nature of electronic transition and is equal to ½ or 2 for direct and indirect transition band gaps respectively.

The measured reflectance spectra can be transformed to the corresponding absorption spectra by applying the Kubelka-Munk function

$$\mathrm{F}(R\infty) = \frac{K}{S} = \frac{(1-R\infty)2}{2R\infty}\ldots\ldots\ldots\ldots\ldots..(3.7)$$

Where $R_\infty = Rsample/Rstandard$ is the reflectance of an infinitely thick specimen, while K and S are the absorption and scattering coefficients respectively. Putting $(R\infty)$ instead of α in equation [3.7] we get,

$$(F(R_\infty).\, h\upsilon)^{\mathbf{1}/\gamma} = \mathrm{B}(h\upsilon - E_g) \;\ldots\ldots\ldots\ldots\ldots.(3.8)\ [35]$$

3.3 Scanning Electron Microscopy

Scanning electron microscope is one of the most versatile or multifaceted instruments which are used to observe the structure morphology at higher magnification and chemical composition characterization.

3.3.1 Principle

The Scanning electron microscope works on the principle of applying kinetic energy to produce signals on the interaction of the electrons. These electrons are secondary electrons, backscattered electrons, and diffracted backscattered electrons which are used to view crystallized elements and photons.

Backscattered electrons: Backscattered electrons are reflected back when the primary electron beams the sample. These are elastic interactions. Backscattered electrons come from deeper areas of samples. Its image displays high sensitivity in difference in atomic numbers which will show up as brighter or darker

Secondary electrons: The secondary electrons are from atoms of the sample and they are inelastic interactions. It comes from surface regions. Scattered electrons give information about the nano and micro structure of the samples in the form of an image. Scintillator is used as a detector which is held at a high positive potential of several KV and the secondary electrons are accelerated into the scintillator to give visible light which is then detected by photomultiplier.

At each point signals are emitted from specimens and are collected by detectors. The detector signal is synchronized with the known location of the beam on the specimen and signal intensity used to modulate the corresponding image pixel. The signals collected in series are combined to form an Image whose dimension distribution depends upon the scan pattern chosen.[36]

3.3.2 Instrumentation

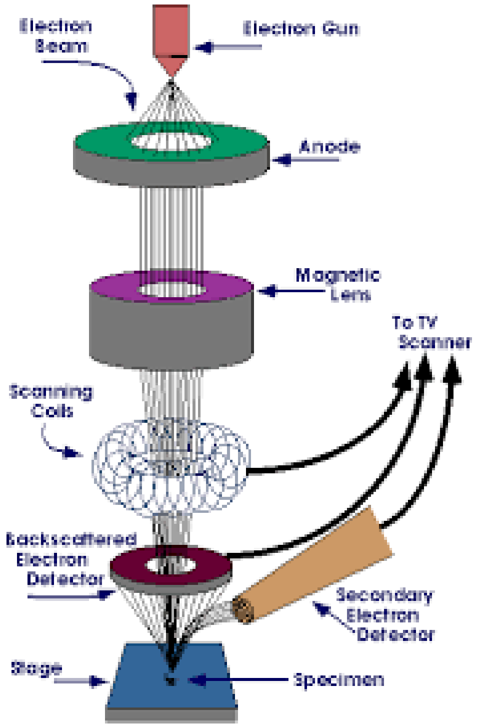

Fig. 3.12 Schematic diagram of a Scanning Electron Microscope.

Adopted from the reference [37]

The scanning electron microscope instrument consists of the following components:

Electron source: The electron source generates electrons at top of the microscope column. The electrons are emitted by heated filament of Tungsten or Lanthanum Hexabromide by thermionic emission.

Anode: Anode has a positive charge, which attracts the electrons to form an electron beam.

Magnetic lens: Magnetic lens controls the size of the beam and determines the number of electrons in the beam. The size of the beam will decide the resolution of the image. Apertures can be also used to control the size of the image.

Scanning coils: The scanning coils deflect the electrons along x and y axes. To ensure it scans in a raster fashion over the surface of the sample.

Objective lens: The objective lens is the last lens among lenses that creates the electron beam.

Since this lens is very close to the sample, it focuses the beam to a very small spot on the sample. Since electrons cannot pass through glass, SEM glass is electromagnetic. They are made up of coils of wire inside metal poles. When current passes through these coils, they generate magnetic fields. Since electrons are highly sensitive to magnetic fields which allows the lenses in the microscope to control them. [37]

3.3.3 Advantages of SEM

Scanning electron microscopy has a broad range of research and practical applications.

- It provides detailed, topographical images, providing versatile data.
- Given proper training, SEM equipment is straightforward to operate, and specialist but user-friendly software supports it. Modern SEM data comes in digital form.
- It is a rapid process, and instruments can complete analysis in under five minutes.
- There is a degree of sample preparation necessary, but usually this is minimal.

3.3.4 Applications

The main application of SEM is for determining materials under high magnification and providing information about sizes, shapes and compositions as seen from solid surfaces. The results complement those obtained from optical microscopy by providing information on submicron-sized features, but can also extend to features up to hundreds of microns across. Images may be recorded using both secondary electrons and back-scattered electrons, with instrumental conditions optimized for good topographic contrast.

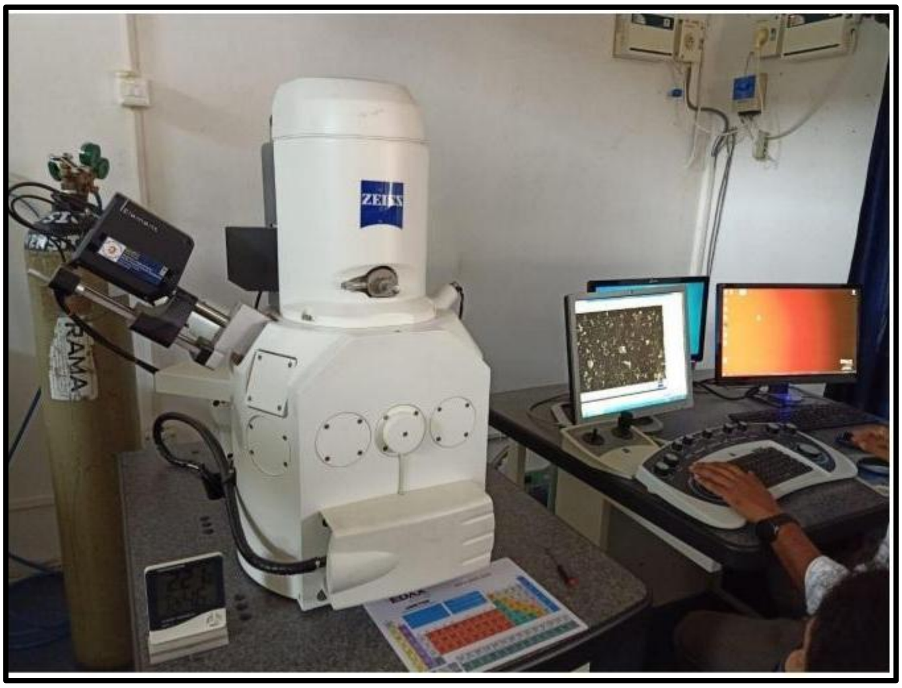

Fig. 3.13: Carl Zeiss Scanning Electron Microscope at USIC of Goa University.

3.4 Photocatalysis

Photocatalysis is a process in which a substance, typically a semiconductor material, known as a photocatalyst, is able to increase the rate of a chemical reaction by absorbing photons of light. When a semiconductor absorbs light energy that has a higher energy than the band gap, an electron is excited from the valence band to the conduction band, leaving behind a hole in the valence band. The excited electron and hole can then participate in various chemical reactions with adsorbed molecules on the surface of the semiconductor, leading to the production of reactive species such as radicals, which can be used for various applications such as environmental remediation and organic synthesis.

Photocatalysts can be used in other types of chemical reactions, such as hydrogen production, carbon dioxide reduction, and organic synthesis.

The photocatalytic reactions can be categorized into two types on the basis of appearance of the physical state of reactants.

Homogeneous photocatalysis: When both the semiconductor and reactant are in the same phase,it can be used for reactions that occur in solution or in the gas phase such photocatalytic reactions are termed as homogeneous photocatalysis.[38]

One of the very common examples of homogeneous photocatalysts used is ozone and photo-Fenton systems (Fe^+ and Fe^+/H_2O_2). Here the reactive species is to be the hydroxyl radical (•OH) which tends to be used for various purposes and objectives. This mechanism of producing hydroxyl radical (•OH) by ozone can follow these two paths mentioned below.

$$O_3 + h\nu \rightarrow O_2 + O(1D)$$

$$O(1D) + H_2O \rightarrow \bullet OH + \bullet OH$$

$$O(1D) + H_2O \rightarrow H_2O_2$$

$$H_2O_2 + h\nu \rightarrow \bullet OH + \bullet OH$$

In the same way, the Fenton system (Fe^+) produce hydroxyl radical (•OH) by the mechanism shown below.

$$Fe^{2+} + H_2O_2 \rightarrow HO\bullet + Fe^{3+} + OH^-$$

$$Fe^{3+} + H_2O_2 \rightarrow Fe^{2+} + HO\bullet 2 + H^+$$

$$Fe^{2+} + HO\bullet \rightarrow Fe^{3+} + OH^-$$

In the photo-Fenton systems (Fe^+ and Fe^+/H_2O_2) type processes, supplemental sources of OH radicals are also considered: via photolysis of H_2O_2, and by the reduction of Fe^{3+} ions under UV light as follows:

$$H_2O_2 + h\nu \rightarrow HO\bullet + HO\bullet$$

$$Fe^{3+} + H_2O + h\nu \rightarrow Fe^{2+} + HO\bullet + H^+$$

The productivity and effectiveness of Fenton type processes is influenced by various operating parameters/variables such as concentration of hydrogen peroxide (H_2O_2), pH as well as intensity of the UV light. The leading edge of this process is the capability of using sunlight with light sensitivity up to 450 nm, hence; saving the process from use of high costs of UV lamps and electrical energy. These type of reactions in homogeneous photocatalysis are proved to be more convenient and economical than the other photocatalysis types, however the major downsides of this process are the low pH values, which are needed, because iron (Fe) precipitates at some higher pH values, furthermore the fact that iron (Fe) has to be eliminated after the treatment.[39]

Heterogeneous photocatalysis: When both the semiconductor and reactant are in different phases,it is typically used for reactions that involve a solid semiconductor and a liquid or gas reactant. Such photocatalytic reactions are classified as heterogeneous photocatalysis.[38]

In general and commonly used heterogeneous photocatalysts include transition metal oxides and semiconductors, which undergo unique characteristics. Contrary to the metals that possess a continuum of electronic states, semiconductors usually have ineffective energy regions where no such energy levels are available to develop rejoining of an electron and a hole produced by photo-activation in the solid substance. The void/ineffective region, which outstretches from the top of the filled valence band to the bottom of the vacant conduction band, is termed as the band gap.The development of new and more efficient photocatalysts is an active area of research in materials science and chemistry, with the goal of finding sustainable and renewable solutions for energy production and environmental protection. [38]

3.4.1 Mechanism of Photocatalysis

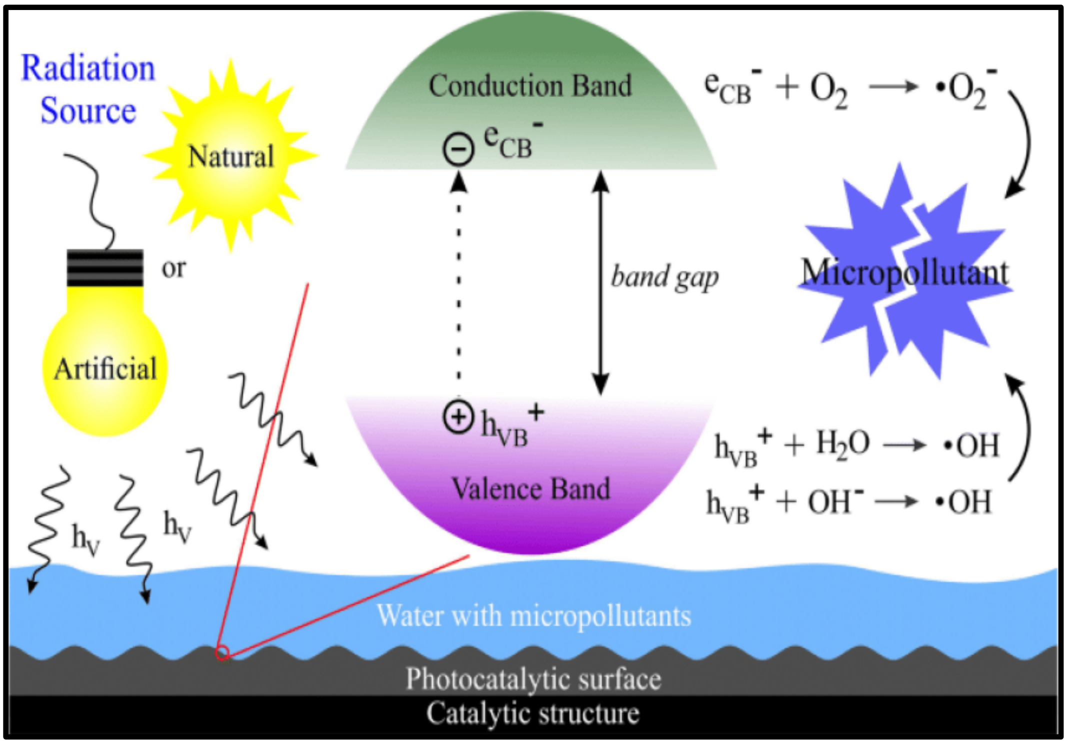

Fig.3.14: Mechanism of Photocatalysis. Adopted from the reference [38]

With the passage of time new and different strategies have been applied. For example surface and interface modification by managing particle size and shape, composite or coupling materials, doping of transition metal, doping of nonmetal, application of co-doping (like; metal–metal, metal–nonmetal, nonmetal–nonmetal), deposition of noble metal, and by the use of organic dye and metal complexes sensitization of surface, in order to enhance and boost the photocatalytic properties.

The process of Photocatalysis can be used with a practical and successful approach in a real earth environment in order to decompose different types of pollutants, and it can enhance the quality of air in the atmosphere. Therefore the process of Photocatalysis can be used in the building and construction industry for the purpose of improving indoor air quality.

In this process a photon with energy equal to or greater than that of the materials band gap is absorbed by the semiconductor used, then an electron excites from the valence band to the conduction band, so it generates a positive (+ve) hole in the valence band. This phenomenon of photo-generated electron-hole pairs is called the ***exciton***. The excited electron and hole can recombine or rejoin and release the energy that they gained when the electron was excited as heat. This Exciton and recombination is not desirable and the higher levels of it take the process to an ineffective photocatalyst. Because of this reason endeavors to flourish and develop functional photocatalysts frequently put an emphasize on extending the exciton lifetime, so that improving electron-hole separation using different approaches that usually depend upon structural characteristics such as phase hetero-junctions (for example; anatase-rutile interfaces), noble-metal nanoparticles, silicon nanowires and substitutional cation doping etc. The main objective of photocatalyst designing is to facilitate and pave the way for reactions between the excited electrons with oxidants to produce reduced products. Additionally in order to make reactions between the holes generated along with the reductants to produce oxidized products. Because of the generation of positive (+ve) holes and electrons, redox reactions occur at the surface of semiconductors.

The mechanism of the oxidative reaction shown below, depicts the positive holes that react with the moisture present on the material's (metal oxide) surface and produce a hydroxyl radical (•OH). This reaction begins with photo-induced exciton-generation in the metal oxide surface (where; MO stands for metal oxide):

$$\mathrm{MO} + h\nu \rightarrow \mathrm{MO}\ (h^{+} + e^{-})$$

Oxidative reactions due to photocatalytic effect are as below:

$$h^{+} + \mathrm{H_2O} \rightarrow \mathrm{H}^{+} + \bullet\mathrm{OH}$$

$$2\ h^{+} + 2\ H_2O \rightarrow 2\ H^{+} + H_2O_2$$

$$H_2O_2 \rightarrow 2\ \bullet OH$$

Reductive reactions due to photocatalytic effect are as below:

$$e^{-} + O_2 \rightarrow \bullet O_2^{-}$$

$$O_2^{-} + H_2O + H^{+} \rightarrow H_2O_2 + O_2$$

$$H_2O_2 \rightarrow 2\ \bullet OH$$

Finally, the generation of hydroxyl radical (•OH) takes place in both reactions mentioned above. Such hydroxyl radical (•OH) are extremely oxidative in nature and non-selective with redox potential of (E_0 = +3.06 V) as well.

3.4.2 Factors affecting photocatalysis

In general terms the oxidation rates and productivity of the photocatalytic systems highly rely on various operational parameters that control the photo-degradation of organic molecules. A number of case studies have reported the significance of these operational parameters. The photo-degradation depends upon some of the basic parameters mentioned below:

a. Concentration of substrate

b. Amount of photocatalyst

c. The pH of solution

d. Temperature of reaction medium

e. Time of irradiation of light

f. The intensity of light

g. Surface area of photocatalyst

h. Dissolve oxygen in the reaction medium

i. Nature of the photocatalyst

j. Nature of the substrate

k. Doping of metal ions and non-metal

l. Structure of photocatalyst and substrate

Hence, the photo-degradation of organic compounds has been studied by a number of scientists and researchers; so a final conclusion is made that the optimum conditions for the photo-degradation of organic compounds must rely upon above parameters.

With the passage of time new and different strategies have been applied. For example surface and interface modification by managing particle size and shape, composite or coupling materials, doping of transition metal, doping of nonmetal, application of co-doping (like; metal–metal, metal–nonmetal, nonmetal–nonmetal), deposition of noble metal, and by the use of organic dye and metal complexes sensitization of surface, in order to enhance and boost the photocatalytic properties.[3]

4. Results and discussion

4.1: X-Ray Diffraction

The PXRD data was collected on the prepared ground sample with 2θ varying from 10^o to 80^o with a step size of 0.02^o using Cu Kα radiation of wavelength 1.5408 Å on the Rigaku SmartLab X-Ray Diffractometer. The collected Data was subjected to the Rietveld refinement using FullProf software.

The Rietveld refinements carried out on the PXRD data indicate that all 6 as-prepared samples have a cubic structure belonging to the Fm-3m space group as reported in literature. Fig.4.1 shows the comparison of XRD patterns. The sharp and intense Bragg peaks indicate that the samples have crystallized very well. The Bragg peaks shift towards lower 2θ values with increasing Sb concentration indicating that the lattice parameter increases with the substitution of Sb in the In sites. The lattice parameters as given in table 4.1 are seen to increase proportionally with increasing Sb concentration further confirming Sb doping.

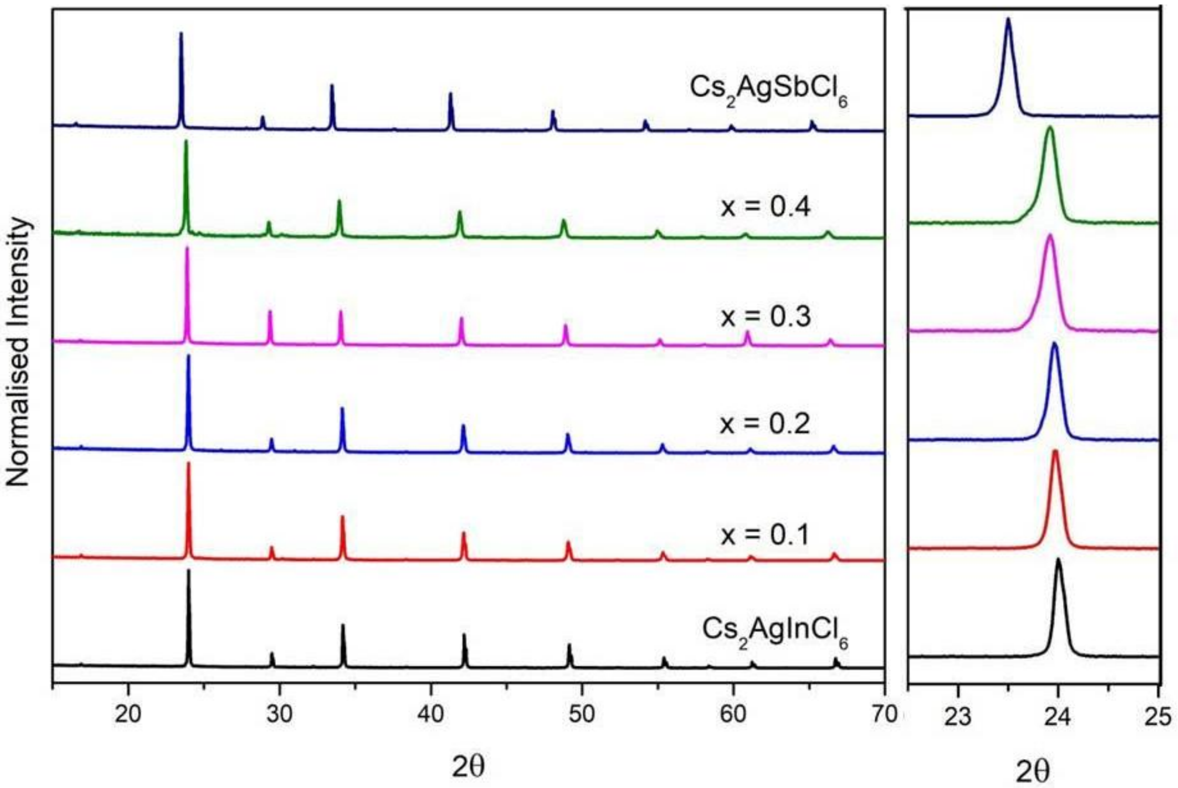

Fig. 4.1: X ray Diffraction Patterns of as prepared $Cs_2AgIn_{(1-x)}Sb_xCl_6$

Table 4.1: Lattice parameters of $Cs_2AgIn_{(1-x)}Sb_xCl_6$

$Cs_2AgIn_{(1-x)}Sb_xCl_6$	**x = 0**	**x = 0.1**	**x = 0.2**	**x = 0.3**	**x = 0.4**	**x = 1**
Lattice parameter (Å)	10.475(3)	10.491(11)	10.505(8)	10.533 (4)	10.578 (9)	10.695 (5)
Unit Cell Volume (Å^3)	1149.47(4)	1,154.81 (9)	1159.30(7)	1168.56 (6)	1183.91 (2)	1223.50 (7)

Rietveld refinement has been shown below for two of the samples namely x=0 and x=0.2

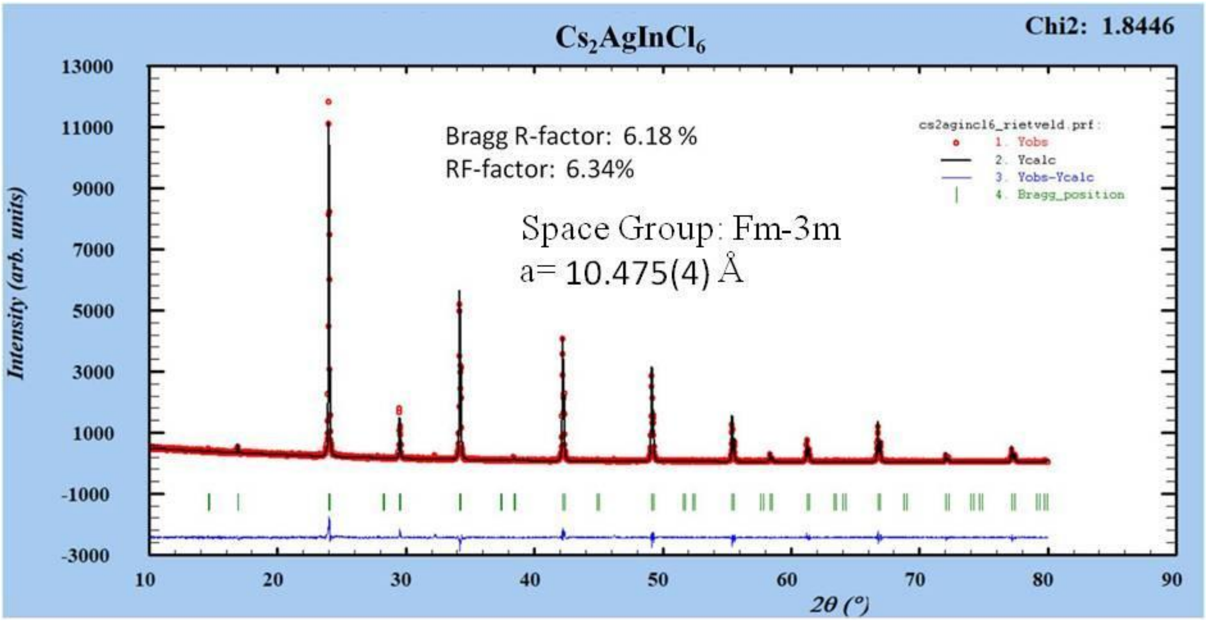

Fig. 4.2: Rietveld refinement of $Cs_2AgInCl_6$

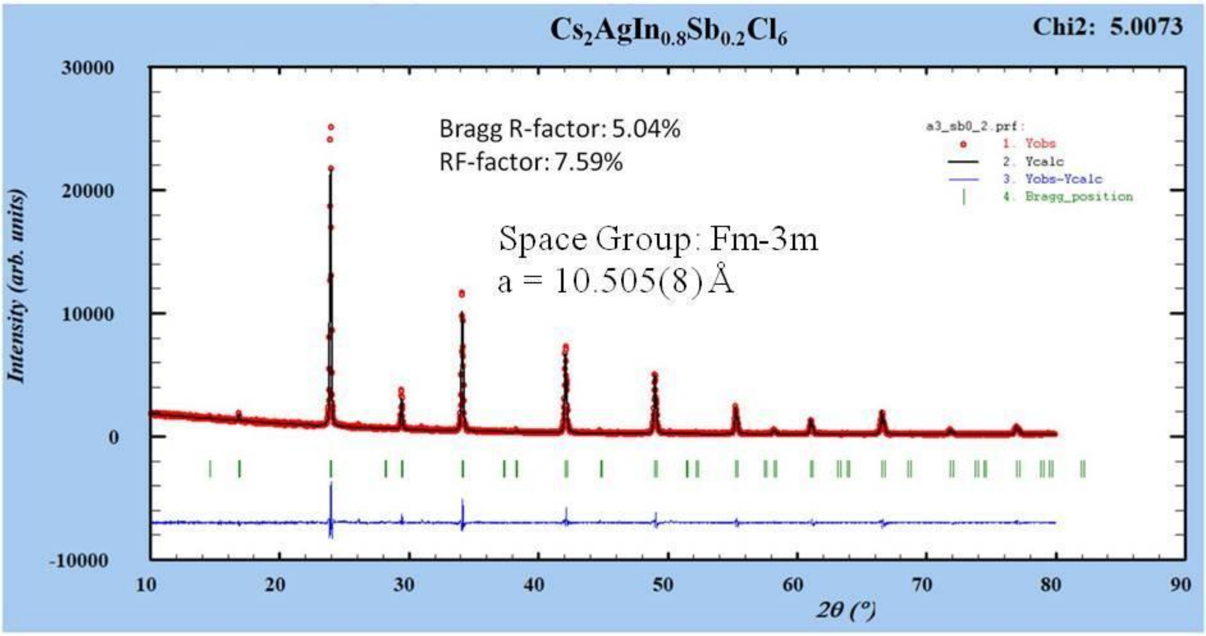

Fig. 4.3: Rietveld refinement of $Cs_2AgIn_{0.8}Sb_{0.2}Cl_6$

4.2 Morphological study

SEM images of as synthesized $Cs_2AgInCl_6$ were taken using Zeiss Scanning Electron Microscope. The crystals were found to be in the range of 3 to 8 µm as can be seen from figures 4.4(a) and 4.4(b). The crystals are octahedral in shape even though the unit cell is face centred cubic as confirmed by PXRD. The octahedral crystal structure is due to preferred stacking of the cubic unit cells (fig. 4.5)

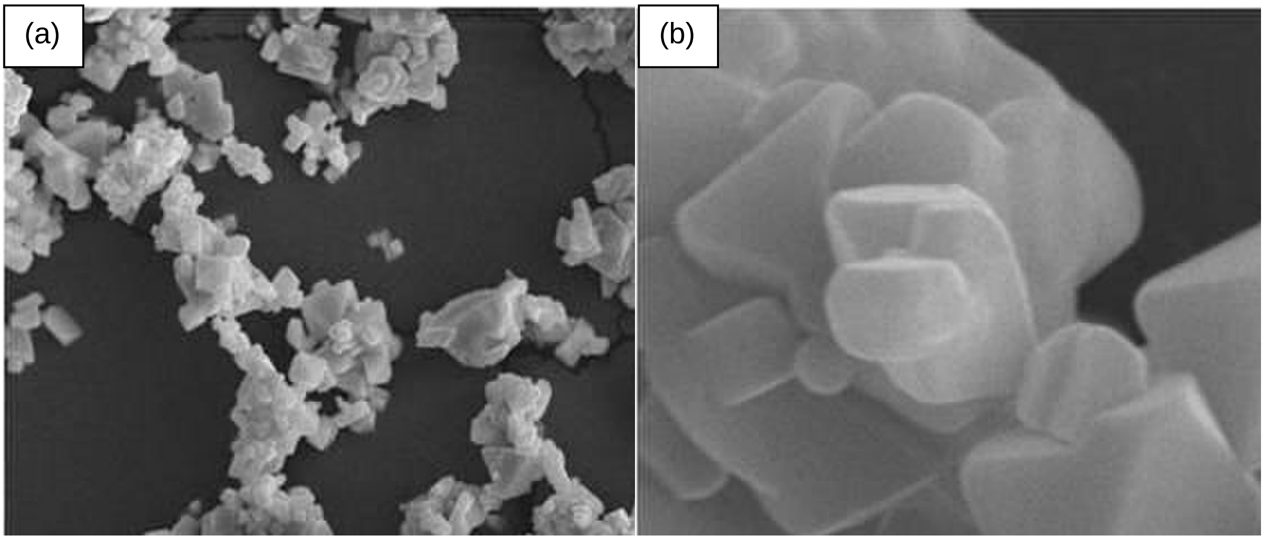

Fig.4.4 SEM image of $Cs_2AgInCl_6$ with scale in fig (a) equal to 10µm and that in (b) equal to 1µm

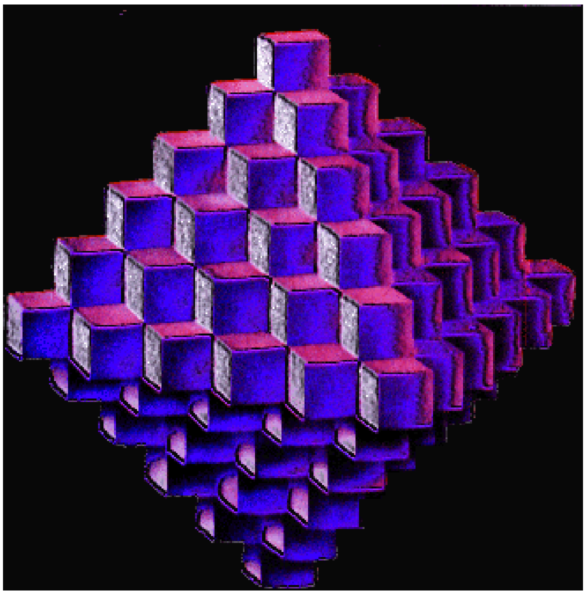

Fig. 4.5 Octahedral stacking of Cubic unit cells of diamond
Adopted from the reference [40]

4.3 UV-Vis Spectroscopy –Band gap study

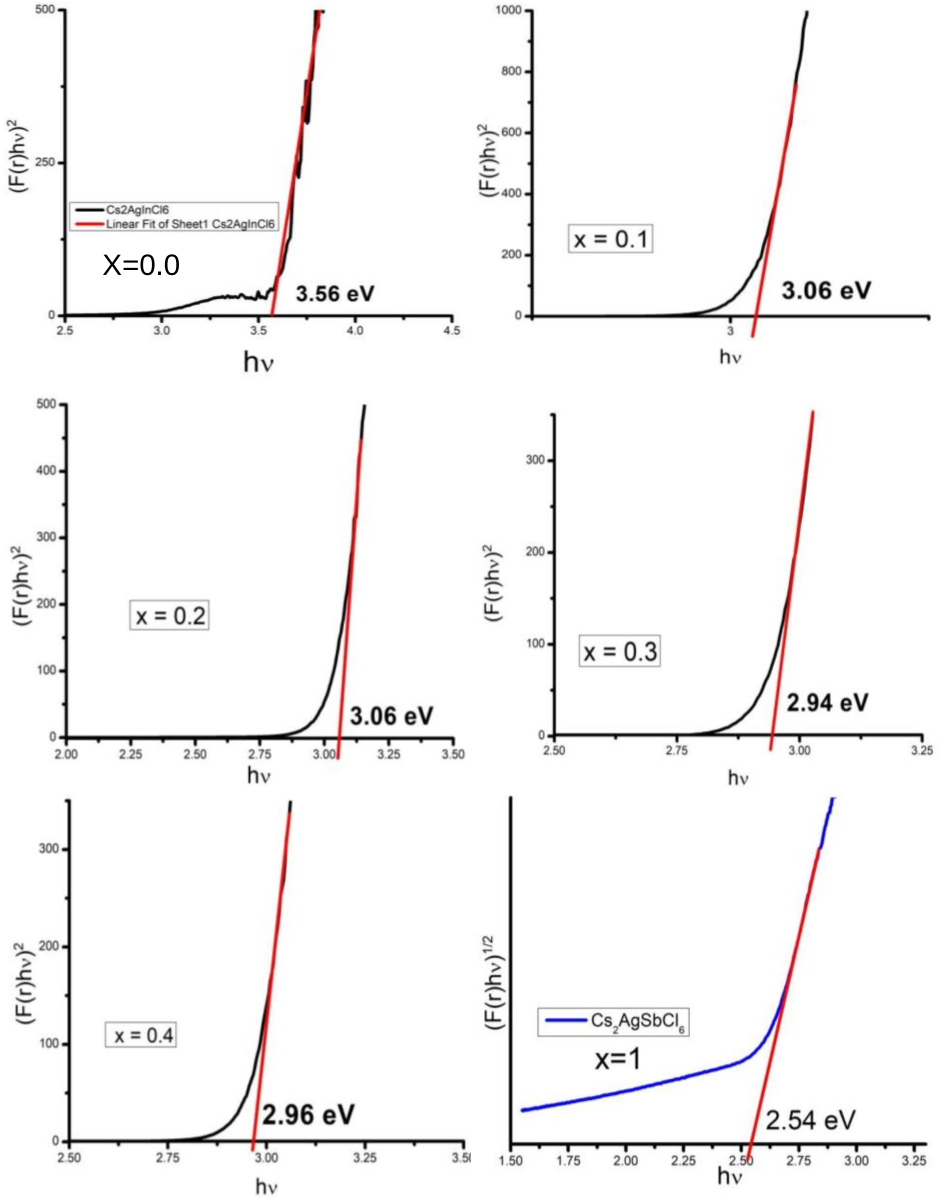

Fig. 4.6 Tauc Plots of $Cs_2AgIn_{(1-x)}Sb_xCl_6$ drawn using data obtained from UV-Vis Diffuse Reflectance Spectroscopy

The UV-Vis DRS Spectra were recorded on Shimadzu UV-Vis spectrophotometer in the range 200 nm to 800 nm. The obtained data was used to plot Tauc plots from which the energy band gap of the compounds were determined. The Tauc plots for samples x=0.0,0.1,0.2,0.3,0.4 were plotted between $(F_{(r)}h\nu)^{\gamma}$ and $h\nu$ with $\gamma = 2$ which gives direct band gap on the extrapolation of absorption edge. The Tauc plots for sample x=1 was plotted between $(F_{(r)}h\nu)^{\gamma}$ and $h\nu$ with $\gamma = 1/2$ which gives indirect band gap. [41]

It is clear from the graphs in fig 4.6 that the samples x=0.0,0.1,0.2,0.3,0.4 possess direct band gap while the sample $Cs_2AgSbCl_6$ possesses indirect band gap. Table 4.2 gives the band gap values which are in good agreement matched with those reported in literature. [42]

Table 4.2: Energy band gaps of $Cs_2AgIn_{(1-x)}Sb_xCl_6$ as calculated from Tauc plots

Compound	**Band Gap in eV**	**Reported value**
$Cs_2AgInCl_6$	3.56	3.53
x = 0.1	3.06	—
x = 0.2	3.06	3.06
x = 0.3	2.94	—
x = 0.4	2.96	2.92
$Cs_2AgSbCl_6$	2.54	2.54

4.4 Photodegradation of organic dyes

The primary aim of the project was to test the prepared samples for photocatalytic applications. Two organic dyes namely Sudan Red III and Methyl Orange were chosen for the photo-degradation experiments. The experiment was carried out in Lelesil UV-Vis photochemical reactor consisting of a 250W UV lamp with a predominant wavelength of 280 nm. To prepare the dye solution 10mg of dye was dissolved in 100ml of solvent which was further diluted 10 times to get 10mg/L solution. The Methyl Orange solution was prepared in distilled water while that of Sudan Red was prepared in ethanol since it does not dissolve in water. 50mg of dye was taken in 100ml dye solution and stirred for 1hour in the dark to reach adsorption desorption equilibrium before turning on the UV lamp. 3ml of this solution was taken out in a quartz cuvette using a syringe and absorbance spectra was recorded from 250nm to 700nm on Shimadzu UV-Vis Spectrophotometer. This step was repeated at thirty minute intervals and the degradation of the dyes was observed. Fig 4.7 shows the absorbance spectra of Sudan Red III solution degraded using $Cs_2AgInCl_6$. The absorbance graphs are similar for other samples as well and hence have not been shown. The characteristic absorption peak for Sudan Red III appears at 503 nm and that for methyl orange exists at 495 nm.

The absorbance decreases with decreasing dye concentration since they are directly proportional to each other. The maximum absorbance occurs at 0 min and the corresponding concentration is taken as 100% concentration or C_0. C_t is the concentration value at time t minutes. The ratio of C_t/C_0 as a function of time has been plotted for all samples and shown in Fig. 4.8.

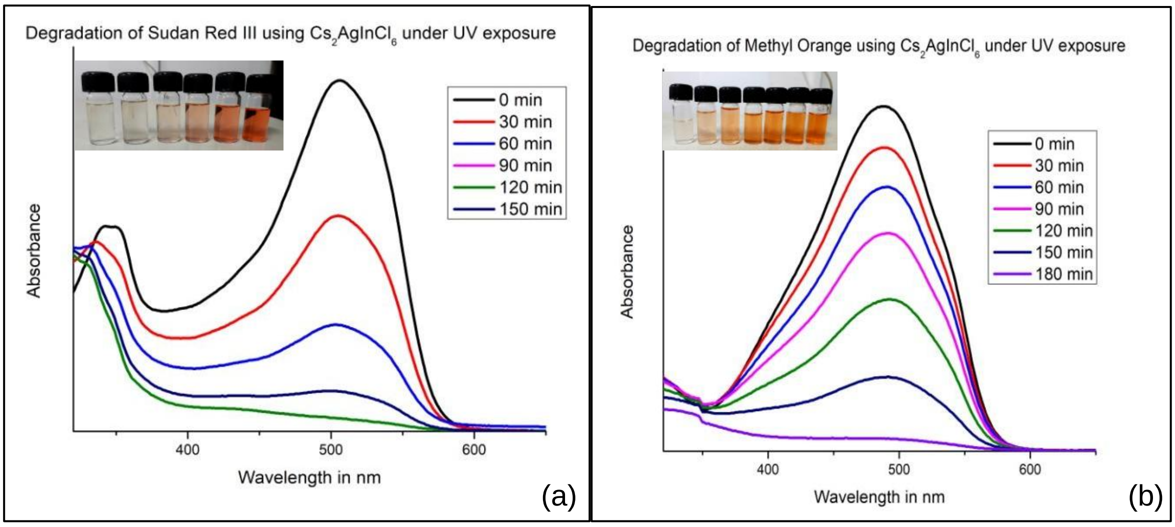

Fig. 4.7 UV–Vis absorption spectra for (a) Sudan Red III and (b) Methyl Orange degradation in the presence of $Cs_2AgInCl_6$ under various UV-light irradiation times (The inset shows the change of solution colour)

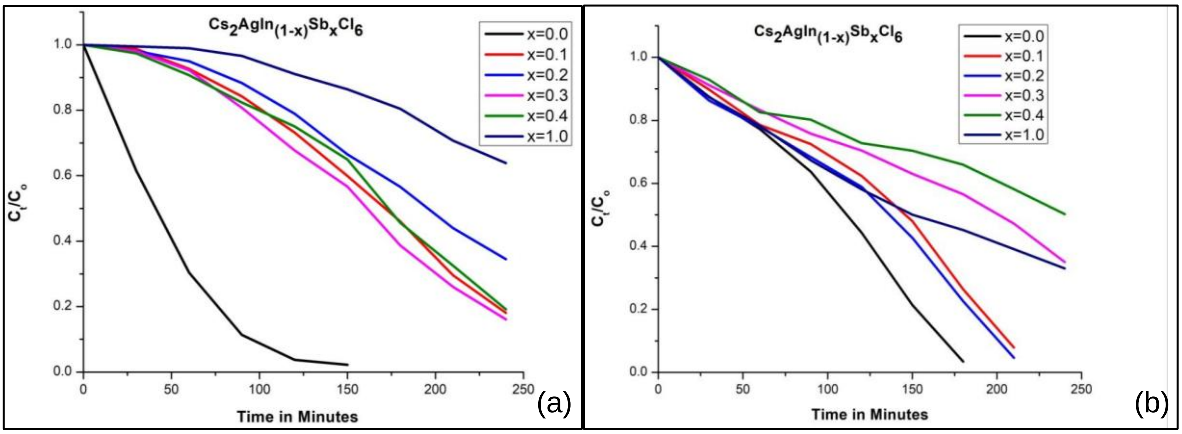

Fig. 4.8 Plots of C_t/C_0 versus the irradiation time for photocatalytic degradation of (a) Sudan Red III and (b) Methyl Orange for $Cs_2AgIn_{(1-x)}Sb_xCl_6$ samples.

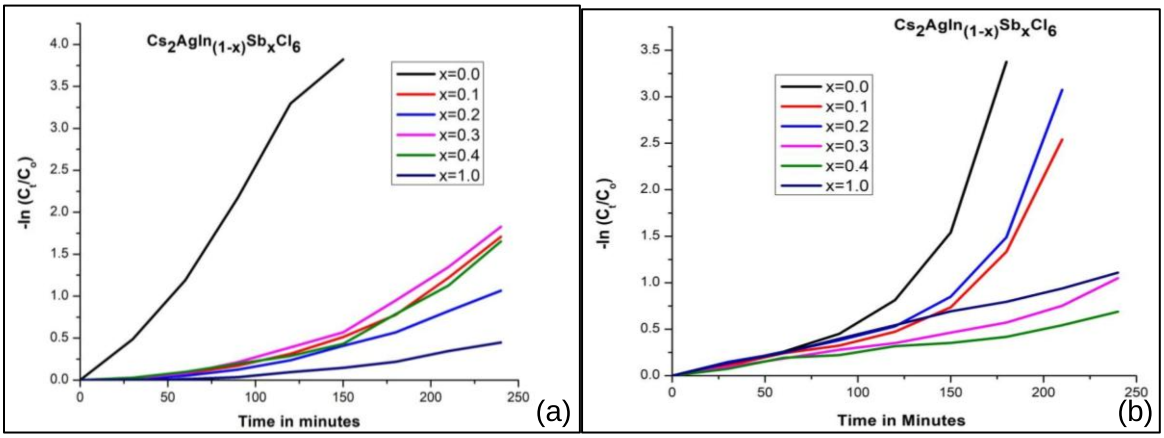

Fig. 4.9 Kinetic curves of photocatalytic degradation reaction for (a) Sudan Red III and (b) Methyl Orange dyes.

It is observed that both dyes degrade faster in the presence of $Cs_2AgInCl_6$ as the catalyst and the degradation rate decreases with increasing Sb Concentration. This can be attributed to the fact that $Cs_2AgInCl_6$ has a direct energy band gap while the incorporation Sb induces an indirect band gap in the compounds [42]

Table 4.3 gives the degradation rate constants of the dyes which are the slopes of the graphs in fig 4.9. These slopes have been calculated by fitting a linear curve through the graphs. Clearly the degradation is maximum and fastest in the presence of $Cs_2agInCl_6$ and decreases with increasing Sb doping at the In site.

Table 4.3: The dye degradation rate constant (k) values of Sudan Red III and Methyl Orange

Compound	**Dye degradation constant (k)**	
	Sudan Red III	**Methyl Orange**
$Cs_2AgInCl_6$	0.027162	0.016063
x = 0.1	0.006777	0.010129
x = 0.2	0.004439	0.011971
x = 0.3	0.007429	0.003961
x = 0.4	0.006402	0.002632
$Cs_2AgSbCl_6$	0.001858	0.004576

5. Summary

- Powdered crystalline samples of $Cs_2AgIn_{(1-x)}Sb_xCl_6$ were prepared using time efficient and simple acid precipitation method.

- The samples were subjected to Rietveld refinement using Fullprof software and found to be phase pure .

- The lattice parameter increases with increasing Sb concentration at the In site in $Cs_2AgInCl_6$ which results in the shift of Bragg peaks towards lower 2θ values in the PXRD graphs

- The compounds crystallize in octahedral shape as seen in SEM images with a face centred cubic unit cell belonging to the Fm-3m space.

- The tauc plots reveal that the energy band gap decreases with increasing Sb concentration. However the nature of this band gap needs to be further investigated since presence of Sb induces an indirect band gap in the compounds.

- The samples exhibit good photocatalytic behavior and were able degrade Sudan Red III and Methyl orange efficiently in the presence of UV light.

- However the photocatalytic property decreases with increasing the Sb concentration in the In site which may be attributed to the presence of indirect band gap upon Sb doping.

Further Investigation

Single crystals of the samples can be prepared to improve purity

The UV Vis spectra must be rerecorded and analysed for nature of band gap

The photocatalytic experiments can be repeated and carried out for more dyes such as Methylene blue and Rhodamine B.

References

1. Malik, A., Grohrmann, E. *Environmental protection strategies for sustainable development.* Strategies for Sustainability, Springer Science & Business Media. 2012.
2. Singh, A., et al. *Toxicology of dyes* Impact of textile dyes on public health and the environment. 2020 p.50-70.
3. Guo, Z., & Chen, J.G. *Photocatalysis and photoelectrocatalysis: Recent advances in materials and potential applications*. ACS Energy Lett. 2017, **2(4)**, p. 906-914.
4. D. L. Bish, J. E. Post. *Modern powder diffraction*. Mineralogical Society of America 1989.
5. Lellis, B., C. Z., et al. *Effects of textile dyes on health and the environment and bioremediation potential of living organisms*. Biotechnol. Res. Innov. 2019 **3(2)**, p.275-290.
6. Cullity, B. D. *Elements of X-ray diffraction*. Addison-Wesley publishing company Inc. 1978.
7. Dann, S. E. *Reactions and characterization of solids.* Royal Society of Chemistry, 2000.
8. Eby, G. N. *Principles of environmental geochemistry*.Thomson, Brooks/Cole.2004
9. Ghasemi E, Kaykhaii M. *Application of Micro-cloud point extraction for spectrophotometric determination of Malachite green, Crystal violet and Rhodamine B in aqueous samples*. Spectrochim Acta A Mol Biomol Spectrosc. 2016 **164**, p. 93.
10. Ghasemi, M., et al. *Lead-free metal-halide double perovskites: From optoelectronic properties to applications*. Nanophotonics, 2020 **1.**
11. Li, K., et al., *Highly-efficient and Stable Photocatalytic Activity of Lead-free Cs2AgInCl6 Double Perovskite for Organic Pollutant Degradation.* J. Colloid Interface Sci. , 2021. **596**: p. 376-383

12. *Diamond Crystal Structure*, Animation. Department of Geological Sciences, University of Texas at Austin. Retrieved from http://www.geo.utexas.edu/courses/347k/redesign/Gem_Notes/Diamond/diam_anim.htm
13. Bouman, D.W. *Spectrometer*. Department of Chemistry, Georgetown University https://bouman.chem.georgetown.edu/S00/handout/spectrometer.htm.
14. LibreTexts. *Analytical Chemistry: Physical Methods in Chemistry and Nano Science*. High Performance Liquid Chromatography. Retrieved from https://chem.libretexts.org/Bookshelves/Analytical_Chemistry/Physical_Methods_in_Chemistry_and_Nano_Science_(Barron)/03%3A_Principles_of_Gas_Chromatography/3.02%3A_High_Performance_Liquid_chromatography
15. Sharma. A., Schulman, S.G., *Introduction to Fluorescence Spectroscopy*. Wiley 1999
16. Siles, P.F. et al. *Tunable charge transfer properties in metal-phthalocyanine heterojunctions* Nanoscale. **8** p.8607–8617.
17. Kogan, I.M. *Khimiia krasitelei [Chemistry of dyes]* 1956. Moscow.
18. Justin T, *UV-Vis spectroscopy: Principle, strengths and limitations, and applications*. Technology Networks. 2021
19. Jena A.K., et al *Halide Perovskite Photovoltaics: Background, Status, and Future Prospects* Chem. Rev. 2019, **119, 5**, 3036–3103
20. Liu X. K, et al *Metal halide perovskites for light-emitting diodes*, Nat. Mater 2021 **20** p.10–21
21. Technology Networks. UV-Vis spectroscopy: Principle, strengths and limitations, and applications.
22. Zhang, L., & Zhao, X. *Carbon nanotubes: Properties and application.* J. Nanosci. Nanotechnol, 2010, **10(6)**, p.3739-3758.

23. Ismail, Muhammad & Akhtar, et al. *Pollution, Toxicity and Carcinogenicity of Organic Dyes and their Catalytic Bio-Remediation*. Current Pharmaceutical Design, 2019, **25**, p.3653-3671.
24. Silu H., et al. *Highly efficient atomically dispersed Co–N active sites in porous carbon for high-performance capacitive desalination of brackish water* J. Mater. Chem. A, 2021, **9,** p.11931-11943.
25. Miyata, Kiyoshi et al. *Lead halide perovskites: Crystal-liquid duality, phonon glass electron crystals, and large polaron formation*. Sci. Adv. 2017, **3,** e1701469.
26. Klug, H. P., and L. E. Alexander. *X-ray diffraction procedures for polycrystalline and amorphous materials*. 1974. Wiley, New York.
27. Macyk, W. *Calculation of Band Gap from reflectance. Journal of physical chemistry letters*. Retrieved from https://www.icmpe.cnrs.fr/spip.php?article594
28. Meyer, E., Mutukwa, D. et al. *Lead-Free Halide Double Perovskites: A Review of the Structural, Optical, and Stability Properties as Well as Their Viability to Replace Lead Halide Perovskites*. Metals, 2018, **8**, p.667.
29. Moore, D. M. and R. C. Reynolds, Jr. *X-Ray diffraction and the identification and analysis of clay minerals*. 1997. Oxford University Press, New York.
30. Ismail, Muhammad et al, *Pollution, Toxicity and Carcinogenicity of Organic Dyes and their Catalytic Bio-Remediation*. Curr. Pharm. Des, 2019, **25**, p.3653-3671.
31. Maysarah S., et al *The Occurrence of Escherichia coli in Groundwater of Bekasi City (Case Study: Jatiluhur, Sumur Batu, and Jatirangga Urban Villages)* IOP Conf. Ser.: Earth Environ. Sci. 2020, **566** 012008
32. Ameta, Rakshit & Ameta, Suresh C. *Advanced Oxidation Processes for Waste Water Treatment*. Emerging Green Chemical Technology. 2018

33. Sada, V.L. *UV-Visible Spectroscopy*. Analytical Chemistry. Retrieved from https://www.chemistry-assignment.com/uv-visible-spectroscopy
34. *Scanning Electron Microscopy* (SEM) Instrumentation. Retrieved from https://www.scimed.co.uk/education/sem-scanning-electronmicroscopy/
35. *SEM principles and applications*. Retrieved from https://microbenotes.com/scanning-electronmicroscope-sem/
36. Tauc, J. *Optical properties and electronic structure of amorphous Ge and Si*, Mater. Res. Bull, 1968, **3**, p.37–46.
37. The Great Soviet Encyclopedia, 3rd Edition (1970-1979).
38. Tran, T.T., et al. *Designing indirect–direct bandgap transitions in double perovskites.* Mater. Horiz., 2017,**4,** p.688-693.
39. Uo, Motohiro & Wada, et al. *Applications of X-ray fluorescence analysis (XRF)* 2014
40. Skoog, et al, *Principles of Instrumental Analysis* Belmont, CA, 2007 Thomson Brooks/Cole. p. 169–173
41. Ashtekar, V.S., et al. *Dye wastewater treatment: removal of reactive dyes using inorganic and organic coagulants* J. Ind. Pollut. Control. 2014, **30(1)**. p.33-42
42. Wagner, H.J., et al. *Purification and characterization of phthalocyanines*. J. Mater. Sci., 1982, **17(10)**, p.2781-2791.